Multihop Optical Wireless Communication Over $\mathcal{F}$-Turbulence Channels and Generalized Pointing Errors With Fog-Induced Fading

Ziyaur Rahman, *Student Member, IEEE*, S. M. Zafaruddin, *Senior Member, IEEE*, and V. K. Chaubey, *Senior Member, IEEE*

***Abstract*—Multihop relaying is a potential technique to mitigate channel impairments in optical wireless communications (OWC). In this paper, multiple fixed-gain amplify-and-forward (AF) relays are employed to enhance the OWC performance under the combined effect of atmospheric turbulence, pointing errors, and fog. We consider a long-range OWC link by modeling the atmospheric turbulence by the Fisher-Snedecor $\mathcal{F}$ distribution, pointing errors by the generalized non-zero boresight model, and random path loss due to fog. We also consider a short-range OWC system by ignoring the impact of atmospheric turbulence. We derive novel upper bounds on the probability density function (PDF) and cumulative distribution function (CDF) of the end-to-end signal-to-noise ratio (SNR) for both short and long-range multihop OWC systems by developing exact statistical results for a single-hop OWC system under the combined effect of $\mathcal{F}$-turbulence channels, non-zero boresight pointing errors, and fog-induced fading. Based on these expressions, we present analytical expressions of outage probability (OP) and average bit-error-rate (ABER) performance for the considered OWC systems involving single-variate Fox's H and Meijer's G functions. Moreover, asymptotic expressions of the outage probability in high SNR region are developed using simpler Gamma functions to provide insights on the effect of channel and system parameters. The derived analytical expressions are validated through Monte-Carlo simulations, and the scaling of the OWC performance with the number of relay nodes is demonstrated with a comparison to the single-hop transmission.**

***Index Terms*—Fisher-Snedecor $\mathcal{F}$ distribution, foggy channel, multihop, non-zero boresight pointing errors, optical wireless communication.**

I. Introduction

OPTICAL wireless communication (OWC) is emerging as a key technology for backhaul connectivity in the next-generation wireless network [1], [2], [3], [4]. The OWC system exploits large unlicensed bandwidth to provide exceedingly higher data rate with low latency transmissions and possesses narrow beam divergence for secured data links without electromagnetic interference. Despite these advantages, the OWC technology is susceptible to atmospheric conditions such as turbulence environment and foggy weather conditions and requires line-of-sight prorogation with near-perfect beam-alignment between the transmitter and detector. Developing efficient techniques to mitigate these channel fading impairments efficiently is desirable for an effective design of OWC systems.

Multi-aperture and cooperative relaying are potential techniques to mitigate the fading effect and extend the communication range. There has been extensive research on relay-assisted OWC systems with regenerative and non-regenerative protocols under the combined effect of atmospheric turbulence and pointing errors. Dual-hop relaying using both decode-and-forward (DF) and amplify-and-forward (AF) protocols is a well-studied topic for optical wireless channels [5], [6], [7], [8]. However, analyzing the performance of multihop relaying is challenging for mathematically complicated turbulence fading models, especially when the AF relaying is employed at each hop. It is known that analyzing DF-assisted multihop system is greatly simplified since the performance analysis decouples into each hop independently and thus requires statistical derivation of a single link [9], [10], [11], [12], [13], [14], [15], [16]. Further, the DF-based multihop requires channel state information (CSI) at each hop and becomes impractical when the number of hops increases beyond a certain limit.

Scanning the literature, there have been studies on the AF relaying for multihop OWC transmissions [9], [17], [18], [19], [20], [21], [22], [23], [24], [25]. Tsiftsis et al. analyzed the exact performance of multihop optical transmission over Gamma-Gamma atmospheric turbulence using channel-assisted AF relaying [9]. However, fixed-gain relaying is desirable due to a simpler implementation but analyzing its performance becomes intractable for many fading channels. To circumvent this, the end-to-end signal-to-noise ratio (SNR) of the fixed-gain multihop AF relaying is upper bounded as the product of SNR of individual links for tractable performance analysis. This approach was first considered in [26] to analyze the multihop relayed communication over Nakagami-m fading channels. Datsikas et al. analyzed the outage probability (OP) and average bit-error-rate (ABER) of an AF-assisted multihop system over Gamma-Gamma atmospheric turbulence without considering

Manuscript received 25 July 2022; revised 8 August 2022; accepted 14 August 2022. Date of publication 19 August 2022; date of current version 13 September 2022. This work was supported in part by the Science and Engineering Research Board, Department of Science and Technology, Government of India under MATRICS under Grant MTR/2021/000890 and in part by Start-Up Research under Grant SRG/2019/002345. *(Corresponding author: Ziyaur Rahman.)*

The authors are with the Department of Electrical and Electronics Engineering, BITS Pilani, Pilani, Rajasthan 333031, India (e-mail: p20170416@pilani.bits-pilani.ac.in; syed.zafaruddin@pilani.bits-pilani.ac.in; vkc@pilani.bits-pilani.ac.in).

Digital Object Identifier 10.1109/JPHOT.2022.3200247

the impact of pointing errors [17]. Tang et al. extended the work presented in [17] considering the combined effect of pointing errors and Gamma-Gamma distributed atmospheric turbulence for the heterodyne OWC system [20]. Zedini and Alouini developed exact and asymptotic analysis for the OP, ABER, and ergodic capacity for an OWC system, pointing errors and atmospheric turbulence. Later, they extended the analysis presented in [19] for the intensity modulation/decision-directed (IM/DD) OWC system [18]. Alheadary et al. considered the misaligned generalized Malaga turbulence and developed ABER performance for the multihop heterodyne OWC system [22]. Ashrafzadeh et al. used the method of induction to develope and exact analysis for an AF-assisted multihop OWC system under the double generalized Gamma turbulence with pointing errors [24], [25].

In the above and related literature, we find a few research gaps in the study of the AF-assisted multihop OWC system, which need to be addressed. Firstly, the AF-assisted multihop transmission was limited to zero-boresight pointing errors and random jitter. The jitter is a random offset of the beam center at the detector plane, and the boresight is the fixed displacement between the center of the beam and the center of the detector [6]. The nonzero boresight model generalizes the effect of pointing errors on the OWC. Although the statistical analysis of nonzero boresight pointing errors for OWC system has been investigated extensively in the literature for single-link, dual-hop, and multi-aperture, it has not been addressed for the AF-assisted multihop transmission. Indeed, there are a few works on the impact of generalized pointing errors but for DF-assisted multihop systems [15], [16].

Secondly, adopted models for atmospheric turbulence were Gamma-Gamma, double generalized Gamma, and Malága distributions. These models are mathematically complicated by including Bessel and Meijer's G-functions in their probability density functions (PDF). Recently, Peppas et al. proposed a new atmospheric turbulence model for OWC, called Fisher-Snedecor $\mathcal{F}$, which provides a better fit for experimental data for all turbulence conditions [27]. Further, the PDF of $\mathcal{F}$ turbulence is more mathematically tractable since it includes elementary functions. There has been an increased interest to analyze the performance of OWC over $\mathcal{F}$ turbulence [28], [29], [30], [31], [32]. However, no work has been reported even with the DF-assisted multihop OWC system considering the $\mathcal{F}$ atmospheric turbulence model.

Thirdly, signal attenuation for OWC transmissions is assumed to be deterministic and quantified using a visibility range, for example, less attenuation in haze and more loss of signal power in foggy conditions. However, recent measurement data confirm that the signal attenuation in foggy weather for terrestrial applications is not deterministic but follows a probabilistic model [33], [34], [35]. The authors in [36], [37] analyzed the single-link performance of the OWC system under the combined effect of fog and pointing errors. Esmail et al. analyzed the OP of a multihop relay system employing the DF protocol (using the cumulative distribution function (CDF) of the SNR for a single link) to mitigate the effect of fog and pointing errors [36]. In our previous work [38], we studied the DF-based dual-hop relaying for the OWC system under the combined effect of random fog, zero-boresight pointing errors, and atmospheric turbulence distributed according to the double generalized gamma. To the best of the authors' knowledge, there are no analyses available for AF-assisted multihop OWC system under the effect of random fog, non-zero boresight pointing errors, and atmospheric turbulence. In Tables I and II, we provide a summary of the state-of-the art research on the multihop OWC system and OWC system with fog-induced fading, respectively.

In this paper, we employ multiple fixed-gain relays in each hop to enhance the OWC performance under the combined effect of atmospheric turbulence, pointing errors, and fog. The major contributions of the proposed work are listed as follows:

- We analyze the end-to-end performance of a fixed-gain AF multihop relayed OWC system considering independent and non-identical (i.ni.d) fading channels in each hop distributed according to the combined statistics of $\mathcal{F}$-turbulence channels, non-zero boresight pointing errors, and fog-induced fading.
- We develop exact statistical results for the direct link of OWC system under the combined effect of atmospheric turbulence, pointing errors, and random fog. We also develop statistical results for a short-range OWC system by ignoring the impact of atmospheric turbulence.
- We derive novel upper bounds on the PDF and CDF of the end-to-end SNR for fixed gain assisted multihop relaying for both short and long-range OWC systems involving single-variate Fox's H and Meijer's G functions.
- We use the derived statistical results to analyze the OP and ABER performance for single-hop and multihop transmissions considering both short and long-range OWC systems.
- We develop diversity order of the considered system by deriving asymptotic expressions of the OP in high SNR region to provide insights on the design aspects of channel and system parameters.
- We use computer simulations to demonstrate the significance of multihop relaying for OWC systems to mitigate the channel impairment compared with the single-hop system.

Notations: $(\cdot)_i$ denotes the i-th hop, $(\cdot)_N$ denotes the N-hop system, $(\cdot)^{\rm SR}$ denotes the short-range OWC system, $(\cdot)^{\rm LR}$ denotes the long-range OWC system, $(\cdot)^{\rm SH}$ denotes the single-hop system, and $(\cdot)^{\rm MH}$ denotes the multihop system. We denote the expectation operator by $\mathbb{E}[\cdot]$, Gamma function by $\Gamma(a) = \int_0^\infty t^{a-1} e^{-t} dt$, upper incomplete Gamma function by $\Gamma(a,t) = \int_t^\infty s^{a-1} e^{-s} ds$, Gaussian Q function by $Q(\gamma) = \frac{1}{\sqrt{2\pi}} \int_\gamma^\infty e^{-\frac{u^2}{2}} du$, Meijer's G-function by $G_{p,q}^{m,n}\left[z \middle| \begin{smallmatrix} (a_k)_{k=1:p} \\ (b_k)_{k=1:q} \end{smallmatrix}\right]$, and the Fox's H-function by $H_{p,q}^{m,n}\left[z \middle| \begin{smallmatrix} (a_k, A_k)_{k=1:p} \\ (b_k, B_k)_{k=1:q} \end{smallmatrix}\right]$.

The rest of this paper is organized as follows. Section II describes the channel models for fog, non-zero boresight pointing errors, and atmospheric turbulence for multihop OWC communication. In Sections III and IV, the performance of long and short-range OWC systems in terms of OP and ABER is presented, respectively. Numerical and simulation results are presented in Section V. Finally, we conclude the findings of this paper in Section VI.

TABLE I
RELATED LITERATURE ON AF-ASSISTED MULTIHOP OWC SYSTEMS

Reference	Detector	Turbulence	Pointing Errors	Fog-Induced Fading
[9]	IM/DD	Gamma-Gamma	No	No
[18]	IM/DD	Gamma-Gamma	No	No
[19]	IM/DD	Gamma-Gamma	Zero boresight	No
[20]	HD	Gamma-Gamma	Zero boresight	No
[21]	HD	Gamma-Gamma	Zero boresight	No
[22]	IM/DD	Malága	Zero boresight	No
[23]	HD	Malága	Zero boresight	No
[26]	IM/DD	Double Generalized Gamma	Zero boresight	No
[This paper]	IM/DD	Fisher-Snedecor $\mathcal{F}$	Non-zero boresight	Yes

TABLE II
RELATED LITERATURE ON OWC SYSTEMS WITH FOG-INDUCED FADING

Reference	System Model	Pointing Errors	Turbulence
[34]	Single-hop	No	No
[35]	Single-hop	No	No
[46]	Single-hop	No	No
[37]	Single-hop	Zero boresight	No
[42]	Single-hop	Zero boresight	Fisher-Snedecor $\mathcal{F}$
[38]	Dual-hop, DF	Zero boresight	Double Generalized Gamma
[36]	Multihop, DF	Zero boresight	No
[This paper]	Single and Multihop, AF	Non-zero boresight	Fisher-Snedecor $\mathcal{F}$

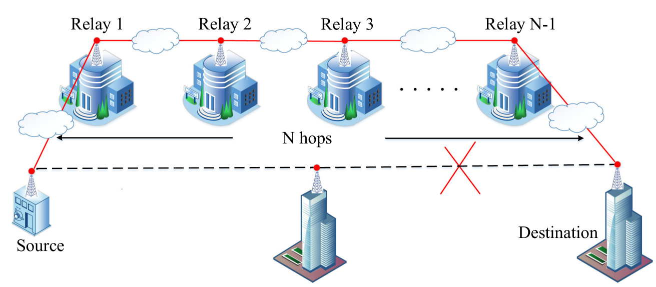

Fig. 1. Multihop OWC communication system.

II. SYSTEM MODEL

We consider an N-hop OWC system where a source terminal communicates with the destination through $N-1$ relay nodes as shown in Fig. 1. The transmitted signal is impaired by the multiplicative channel effects of atmospheric turbulence, pointing error, and random fog. Thus, the received signal y_i for the i-th hop under the additive noise w_i with variance $\sigma^2_{w_i}$ is given by

$$y_i = h_i s + w_i, \tag{1}$$

where s is the transmitted signal and $h_i = h_{f_i} h_{p_i} h_{t_i}$ is the channel coefficient of the i-th hop. Here, h_{f_i} denotes the random fog, h_{p_i} denotes the pointing error, h_{t_i} denote the atmospheric turbulence. We use the simpler non-coherent intensity modulation/direct detection (IM/DD) scheme since heterodyne detection (HD) requires complex processing of mixing the received signal with a coherent signal produced by the local oscillator. Assuming IM/DD technique and on-off keying (OOK) modulation with $x \in \{0, \sqrt{2P_i}\}$ and P_i as the average transmitted optical power, the instantaneous received electrical SNR for the i-th hop is given by [39]

$$\gamma_i^{\mathrm{SH}} = \frac{2P_i^2 h_i^2}{\sigma^2_{w_i}} = \bar{\gamma}_i h_i^2 \tag{2}$$

where $\bar{\gamma}_i$ is the average SNR of the i-th hop. Employing AF relaying with fixed-gain in each hop, the SNR of the N-hop system is given by [40]:

$$\gamma^{\mathrm{MH}}_{\gamma_N} = \left(\sum_{i=1}^{N} \prod_{j=1}^{i} \frac{C_j - 1}{\gamma_j} \right)^{-1} \tag{3}$$

where γ_j is the SNR of j-th hop, and C_j is a positive constant ($C_0 = 1$) depending on the AF gain of the j-th relay. Since the SNR expression in (3) is intractable for statistical analysis, we use a popular upper bound on γ_N [18]:

$$\gamma_N^{\mathrm{MH}} = \frac{1}{N} \prod_{i=1}^{N} C_i^{-\frac{(N-i)}{N}} \gamma_i^{\frac{N+1-i}{N}} \tag{4}$$

If we substitute $N = 1$ in (4), then the SNR of a multihop system becomes the SNR of a single hop system, as depicted in (2) (i.e., $\gamma_N^{\mathrm{MH}} = \gamma_i^{\mathrm{SH}}$ if $N = 1$).

To analyze the statistical performance of the single-hop system in (2) and the multihop system in (4), we require density functions of the foggy channel, atmospheric turbulence, and pointing errors, which are represented in the following.

The probability density function (PDF) of the foggy channel is given as [35]:

$$f_{h_{f_i}}(x) = \frac{z_i^{k_i}}{\Gamma(k_i)} \left(\log \frac{1}{x} \right)^{k_i - 1} x^{z_i - 1}, \; 0 < x \leq 1 \tag{5}$$

where $z_i = 4.343/\beta_{\mathrm{i}} \mathrm{d}_{\mathrm{i}}$, d_i is the distance between the transmitter and receiver of the i-th hop, $k_i > 0$ and $\beta_i > 0$ are the shape parameter and the scale parameter of the fog, respectively.

Next, we consider the Rician distribution to model non-zero boresight and random jitter of the pointing error h_{p_i} [6], [41]

$$f_{h_{p_i}}(x) = \frac{\rho_i^2 \exp\left(\frac{-s_i^2}{2\sigma_i^2}\right)}{A_i^{\rho_i^2}} x^{\rho_i^2-1} I_0\left(\frac{s_i}{\sigma_i^2}\sqrt{\frac{w_{z_{\mathrm{eq_i}}}^2 \ln\frac{A_i}{x}}{2}}\right) \quad (6)$$

where $0 \le x \le A_i$, $I_0(\cdot)$ is the zeroth-order modified Bessel function of the first kind [42], Eq. 8.431.1], $w_{z_{\mathrm{eq_i}}}^2 = \frac{w_{z_i}^2\sqrt{A_i\pi}}{2v_i\exp(-v_i^2)}$, $A_i = [\mathrm{erf}(v_i)]^2$ with $v_i = \sqrt{\frac{r_i^2\pi}{2w_{z_i}^2}}$ as the ratio of aperture radius r_i and beamwidth w_{z_i}, and $\rho_i = \frac{w_{z_{\mathrm{eq_i}}}}{2\sigma_i}$ with σ_i as the standard deviation of the jitter and equivalent beamwidth $w_{z_{\mathrm{eq_i}}}$. Here, $s_i = \sqrt{\mu_{x_i}^2 + \mu_{y_i}^2} \neq 0$ models the non-zero boresight, where $\mu_{x_i} \neq 0$ and $\mu_{y_i} \neq 0$ denote the horizontal and vertical displacement between the center of the beam and the center of the detector, respectively. Note that the model in (6) is a generalized one resulting in the special case of zero boresight with $s_i = 0$ [39].

Finally, we model the atmospheric turbulence channel h_{t_i} using the $\mathcal{F}$-distribution model [27]:

$$f_{h_{t_i}}(x) = \frac{a_i^{a_i}(b_i-1)^{b_i} x^{a_i-1}}{\beta(a_i,b_i)(b_i-1)^{a_i+b_i}(B_i x+1)^{a_i+b_i}} \quad (7)$$

where $0 < x < \infty$, $B_i = \frac{a_i}{(b_i-1)}$, $\beta(\cdot)$ denotes the Beta function, a_i, and b_i are the atmospheric refractive-index structure parameters. The atmospheric refractive-index structure parameters $a_i = \frac{1}{\exp(\sigma_{\ln S_i}^2)-1}$ and inner and outer scale parameter of turbulence $b_i = \frac{1}{\exp(\sigma_{\ln L_i}^2)-1} + 2$ depends on the small-scale $\sigma_{\ln S_i}^2$ and large-scale $\sigma_{\ln L_i}^2$ log-irradiance variances.

In what follows, we analyze the performance of single-hop and multihop OWC system using the combined statistical characterization of fog, non-zero boresight pointing errors, and atmospheric turbulence, as given in (5), (6), and (7), respectively. We analyze the single-hop system since it can have simplified expressions (requiring lesser computation time) than the multihop system. The single-hop system can also become a benchmark for the multihop system, validating the analytical expressions of the multihop system with $N = 1$. Note that the proposed analysis for the single-hop system with the generalized channel model is novel, and the existing (reported in the literature) single-link systems become a particular case of the considered model.

III. Long-Range OWC System

In this section, we analyze the performance of single-hop and multihop OWC systems under the combined effect of atmospheric turbulence, pointing errors, and fog-induced fading. This is a generalized scenario where the statistical impact of all three channel impairments is considered for a better performance assessment. It is argued that fog and turbulence are inversely correlated [39], and thus the presence of one precludes the existence of the other. However, when the density of fog is not high, and the communication range is long, the impact of atmospheric turbulence cannot be ignored.

To proceed with the statistical derivation, first, we find the PDF of $\mathcal{F}$-turbulence channel combined with the non-zero boresight pointing errors $h_{tp,i} = h_{p_i}h_{t_i}$, and then include the foggy component to find the resultant PDF for the channel coefficient $h_i^{\mathrm{LR}} = h_{tp,i}h_{f_i}$. Further, we use the series expansion of modified Bessel function $I_0(x) = \sum_{j=0}^{\infty}\frac{(\frac{x}{2})^{2j}}{(j!)^2}$ in (6) to get

$$f_{h_{p_i}}(x) = \frac{\rho_i^2 \exp\left(\frac{-s_i^2}{2\sigma_i^2}\right)}{A_i^{\rho_i^2}} \sum_{j=0}^{\infty}\frac{1}{(j!)^2} \left(\frac{s_i^2\, w_{z_{\mathrm{eq_i}}}^2}{8\sigma_i^4}\right)^j x^{\rho_i^2-1}\left(\ln\frac{A_i}{x}\right)^j \quad (8)$$

Note that the converging series expansion in (8) facilitates in analyzing the system performance.

A. PDF and CDF of SNR

Lemma 1: The PDF and CDF of SNR for a single-hop OWC system with the combined effect of $\mathcal{F}$-turbulence channels, fog-induced fading and generalized pointing errors are given as:

$$f_{\gamma_i}^{\mathrm{LR}}(\gamma) = \frac{a_i^{a_i} z_i^{k_i}\rho_i^2 \exp\left(\frac{-s_i^2}{2\sigma_i^2}\right)}{2A_i^{a_i}\beta(a_i,b_i)(b_i-1)^{a_i}\sqrt{\gamma\bar{\gamma}_i}} \sum_{j=0}^{\infty}\frac{1}{j!} \left(\frac{s_i^2\, w_{z_{\mathrm{eq_i}}}^2}{8\sigma_i^4}\right)^j \left(\sqrt{\frac{\gamma}{\bar{\gamma}_i}}\right)^{a_i-1} G_{2+j+k_i,2+j+k_i}^{2+j+k_i,1}\left[\begin{matrix}1-a_i-b_i, \{1+\rho_i^2-a_i\}_0^{j+1}, \{1+z_i-a_i\}_1^{k_i}\\ 0, \{\rho_i^2-a_i\}_0^{j+1}, \{z_i-a_i\}_1^{k_i}\end{matrix}\middle| \frac{B_i}{A_i}\sqrt{\frac{\gamma}{\bar{\gamma}_i}}\right] \quad (9)$$

$$F_{\gamma_i}^{\mathrm{LR}}(\gamma) = \frac{a_i^{a_i} z_i^{k_i}\rho_i^2 \exp\left(\frac{-s_i^2}{2\sigma_i^2}\right)}{A_i^{a_i}\beta(a_i,b_i)(b_i-1)^{a_i}} \sum_{j=0}^{\infty}\frac{1}{j!} \left(\frac{s_i^2\, w_{z_{\mathrm{eq_i}}}^2}{8\sigma_i^4}\right)^j \left(\sqrt{\frac{\gamma}{\bar{\gamma}_i}}\right)^{a_i} G_{3+j+k_i,3+j+k_i}^{2+j+k_i,2}\left[\begin{matrix}1-a_i-b_i, 1-a_i, \{1+\rho_i^2-a_i\}_0^{j+1}, \{1+z_i-a_i\}_1^{k_i}\\ 0, \{\rho_i^2-a_i\}_0^{j+1}, \{z_i-a_i\}_1^{k_i}, -a_i\end{matrix}\middle| \frac{B_i}{A_i}\sqrt{\frac{\gamma}{\bar{\gamma}_i}}\right] \quad (10)$$

Proof: See Appendix A. ■

It can be seen that (9) and (10) generalizes the analysis presented in [43] for zero boresight pointing errors. Further, standard functions are available in MATLAB and MATHEMATICA to compute Meijer's G function.

For ease of presentation, we denote $\phi_i = N + 1 - i$ and $\psi_i = C_i^{-\frac{(N-i)}{N}}$ in (4), and use the method described in [44] for terahertz (THz) multihop system to develop the PDF of SNR for N-hop OWC system:

$$f_{\gamma_N}(\gamma) = \frac{1}{\gamma}\frac{1}{2\pi\jmath}\int_{\mathcal{L}}\frac{1}{N}\prod_{i=1}^{N}\psi_i\mathbb{E}[\gamma_i^u]\gamma^{-u}du \quad (11)$$

where $\mathbb{E}[\gamma_i^u]$ is the u-th moment of the SNR for the i-th hop given by

$$\mathbb{E}[\gamma_i^u] = \int_0^\infty \gamma^{u\frac{\phi_i}{N}} f_{\gamma_i}(\gamma) d\gamma \tag{12}$$

Theorem 1: The PDF and CDF of SNR for a multihop OWC system with the combined effect of $\mathcal{F}$-turbulence channels, fog-induced fading and generalized pointing errors are given as:

$$f_{\gamma_N}^{\mathrm{LR}}(\gamma) = \prod_{i=1}^{N} \frac{\psi_i a_i^{a_i} z_i^{k_i} \rho_i^2 \exp\left(\frac{-s_i^2}{2\sigma_i^2}\right)}{N\gamma B_i^{a_i} \beta(a_i,b_i)(b_i-1)^{a_i}} \sum_{j=0}^{\infty} \frac{1}{j!} \left(\frac{s_i^2\, w_{z_{\mathrm{eq_i}}}^2}{8\sigma_i^4}\right)^j H_{2+j+k_i,2+j+k_i}^{2+j+k_i,1} \left[\begin{matrix}(1-b_i, 2\frac{\phi_i}{N}), \{(1+\rho_i^2, 2\frac{\phi_i}{N})\}_0^{j+1}, \{(1+z_i, 2\frac{\phi_i}{N})\}_1^{k_i} \\ \{(\rho_i^2, 2\frac{\phi_i}{N})\}_0^{j+1}, \{(z_i, 2\frac{\phi_i}{N})\}_1^{k_i}, (a_i, 2\frac{\phi_i}{N})\end{matrix} \middle| \prod_{i=1}^{N} \left(\frac{B_i}{A_i\sqrt{\bar{\gamma}_i}}\right)^{2\frac{\phi_i}{N}} \gamma \right] \tag{13}$$

$$F_{\gamma_N}^{\mathrm{LR}}(\gamma) = \prod_{i=1}^{N} \frac{\psi_i a_i^{a_i} z_i^{k_i} \rho_i^2 \exp\left(\frac{-s_i^2}{2\sigma_i^2}\right)}{N B_i^{a_i} \beta(a_i,b_i)(b_i-1)^{a_i}} \sum_{j=0}^{\infty} \frac{1}{j!} \left(\frac{s_i^2\, w_{z_{\mathrm{eq_i}}}^2}{8\sigma_i^4}\right)^j H_{3+j+k_i,3+j+k_i}^{2+j+k_i,2} \left[\begin{matrix}(1,1),(1-b_i, 2\frac{\phi_i}{N}), \{(1+\rho_i^2, 2\frac{\phi_i}{N})\}_0^{j+1}, \{(1+z_i, 2\frac{\phi_i}{N})\}_1^{k_i} \\ \{(\rho_i^2, 2\frac{\phi_i}{N})\}_0^{j+1}, \{(z_i, 2\frac{\phi_i}{N})\}_1^{k_i}, (a_i, 2\frac{\phi_i}{N}), (0,1)\end{matrix} \middle| \prod_{i=1}^{N} \left(\frac{B_i}{A_i\sqrt{\bar{\gamma}_i}}\right)^{2\frac{\phi_i}{N}} \gamma \right] \tag{14}$$

Proof: See Appendix B.

The PDF and CDF of the multihop system in Theorem 1 have a complex representation. However, the PDF of the simpler single-hop system can be used to validate the PDF of the multihop system analytically using $N=1$ in (13). The steps are as follows: With $N=i$ in (13), $\phi_i=1$. Next, we apply the identity $H_{p,q}^{m,n}\left[\begin{matrix}(\alpha_1,C),\ldots,(\alpha_p,C)\\(\beta_1,C),\ldots,(\beta_q,C)\end{matrix}\middle| z\right] = \frac{1}{C}G_{p,q}^{m,n}\left[\begin{matrix}\alpha_1,\ldots,\alpha_p\\\beta_1,\ldots,\beta_q\end{matrix}\middle| z^{\frac{1}{C}}\right]$, $C>0$, [45], p. 50, Eq. 20] to get

$$f_{\gamma_{N=i}}^{\mathrm{LR}}(\gamma) = \frac{\psi_i a_i^{a_i} z_i^{k_i} \rho_i^2 \exp\left(\frac{-s_i^2}{2\sigma_i^2}\right)}{2\gamma B_i^{a_i} \beta(a_i,b_i)(b_i-1)^{a_i}} \sum_{j=0}^{\infty} \frac{1}{j!} \left(\frac{s_i^2\, w_{z_{\mathrm{eq_i}}}^2}{8\sigma_i^4}\right)^j G_{2+j+k_i,2+j+k_i}^{2+j+k_i,1} \left[\begin{matrix}c1-b_i, \{1+\rho_i^2\}_0^{j+1}, \{1+z_i\}_1^{k_i} \\ a_i, \{\rho_i^2\}_0^{j+1}, \{z_i\}_1^{k_i}\end{matrix} \middle| \frac{B_i}{A_i}\sqrt{\frac{\gamma}{\bar{\gamma}_i}}\right] \tag{15}$$

Finally, we apply the identity $G_{p,q}^{m,n}\left[\begin{matrix}a_1,\ldots,a_n,a_{n+1},\ldots,a_p\\b_1,\ldots,b_m,b_{m+1},\ldots,b_q\end{matrix}\middle| z\right] = z^{-\alpha}G_{p,q}^{m,n}\left[\begin{matrix}\alpha+a_1,\ldots,\alpha+a_n,\alpha+a_{n+1},\ldots,\alpha+a_p\\\alpha+b_1,\ldots,\alpha+b_m,\alpha+b_{m+1},\ldots,\alpha+b_q\end{matrix}\middle| z\right]$, [46], Eq. 07.34.17.0011.01] in (15) with $\alpha=-a_i$ and simplify to get the PDF for the single-hop OWC system in (9).

B. Outage Probability

Outage probability is defined as the probability that the instantaneous SNR γ falls below a certain threshold SNR γ_{th} and is given as

$$P_{\mathrm{out}} = P(\gamma < \gamma_{\mathrm{th}}) = F_\gamma(\gamma_{\mathrm{th}}) \tag{16}$$

Substituting (10) in (16), we can get OP for the single-hop transmissions. We can apply the series expansion of Meijer's G function to derive the asymptotic expression for the OP in high SNR regime $\bar{\gamma}_i \to \infty, \forall i$:

$$OP_i^{\mathrm{LR},\infty} = \frac{a_i^{a_i} z_i^{k_i} \rho_i^2 \exp\left(\frac{-s_i^2}{2\sigma_i^2}\right)}{A_i^{a_i}\beta(a_i,b_i)(b_i-1)^{a_i}} \sum_{j=0}^{\infty} \frac{1}{j!}\left(\frac{s_i^2\, w_{z_{\mathrm{eq_i}}}^2}{8\sigma_i^4}\right)^j \left(\sqrt{\frac{\gamma_{\mathrm{th}}}{\bar{\gamma}_i}}\right)^{a_i} \sum_{j'=1}^{2+j+k_i} \frac{\prod_{i'=1,i'\neq j'}^{2+j+k_i}\Gamma(\mathcal{V}_{i'}-\mathcal{V}_{j'})\Gamma(a_i+b_i+\mathcal{V}_{j'})\Gamma(a_i+\mathcal{V}_{j'})}{\prod_{i'=3}^{3+j+k_i}\Gamma(\mathcal{U}_{i'}-\mathcal{V}_{j'})\Gamma(1+a_i+\mathcal{V}_{j'})} \left(\frac{B_i}{A_i}\sqrt{\frac{\gamma_{\mathrm{th}}}{\bar{\gamma}_i}}\right)^{\mathcal{V}_{j'}} \tag{17}$$

where $\mathcal{U}_i' = \mathcal{U}_j' = \{1-a_i-b_i, 1-a_i, \{1+\rho_i^2-a_i\}_0^{j+1}, \{1+z_i-a_i\}_1^{k_i}\}$ and $\mathcal{V}_i' = \mathcal{V}_j' = \{0, \{\rho_i^2-a_i\}_0^{j+1}, \{z_i-a_i\}_1^{k_i}, -a_i\}$. Compiling the exponent of $\bar{\gamma}_i = \bar{\gamma}, \forall i$, the diversity order is derived as $DO_i^{\mathrm{LR}} = \min\{\frac{z_i}{2}, \frac{\rho_i^2}{2}, \frac{a_i}{2}\}$. Note that the diversity order is independent of the boresight parameters.

Similarly, we can substitute the CDF (as given in (14)) of multihop link in (16) to get the OP for the short-range multihop transmissions. We can apply the series expansion of single-varite Fox's H function [47], Eq. 1.8.4] to derive the asymptotic expression for the OP in high SNR regime $\bar{\gamma}_i \to \infty, \forall i$:

$$OP_N^{\mathrm{LR},\infty} = \prod_{i=1}^{N} \frac{\psi_i a_i^{a_i} z_i^{k_i} \rho_i^2 \exp\left(\frac{-s_i^2}{2\sigma_i^2}\right)}{N B_i^{a_i} \beta(a_i,b_i)(b_i-1)^{a_i}} \sum_{j=0}^{\infty} \frac{1}{j!} \left(\frac{s_i^2\, w_{z_{\mathrm{eq_i}}}^2}{8\sigma_i^4}\right)^j \sum_{j'=1}^{2+j+k_i} \frac{1}{\mathcal{S}_{j'}} \frac{\prod_{i'=1,i'\neq j'}^{2+j+k_i}\Gamma\left(\mathcal{R}_{i'}-\mathcal{R}_{j'}\frac{\mathcal{S}_{i'}}{\mathcal{S}_{j'}}\right)\Gamma\left(1-\mathcal{P}_{i'}+\mathcal{R}_{j'}\frac{\mathcal{Q}_{i'}}{\mathcal{S}_{j'}}\right)}{\prod_{i'=2}^{2+j+k_i}\Gamma\left(\mathcal{P}_{i'}-\mathcal{R}_{j'}\frac{\mathcal{Q}_{i'}}{\mathcal{S}_{j'}}\right)\Gamma\left(1+\frac{\mathcal{R}_{j'}}{\mathcal{S}_{j'}}\right)} \left(\prod_{i=1}^{N}\left(\frac{B_i}{A_i\sqrt{\bar{\gamma}_i}}\right)^{2\frac{\phi_i}{N}} \gamma_{\mathrm{th}}\right)^{\frac{\mathcal{R}_{j'}}{\mathcal{S}_{j'}}} \tag{18}$$

where $\mathcal{P}_{i'} = \mathcal{P}_{j'} = \{1, 1-b_i, \{1+\rho_i^2\}_0^{j+1}, \{1+z_i\}_1^{k_i}\}$, $\mathcal{Q}_{i'} = \mathcal{Q}_{j'} = \{1, 2\frac{\phi_i}{N}, \{2\frac{\phi_i}{N}\}_0^{j+1}, \{2\frac{\phi_i}{N}\}_1^{k_i}\}$, $\mathcal{R}_{i'} = \mathcal{R}_{j'} =$

$\{\{\rho_i^2\}_0^{j+1}, \{z_i\}_1^{k_i}, a_i, 0\}$, and $\mathcal{S}_{i'} = \mathcal{S}_{j'} = \{\{2\frac{\phi_i}{N}\}_0^{j+1}, \{2\frac{\phi_i}{N}\}_1^{k_i}, 2\frac{\phi_i}{N}, 1\}$. Similarly, the diversity order is given as $DO_N^{\mathrm{LR}} = \sum_{i=1}^N \min\{\frac{z_i}{2}, \frac{\rho_i^2}{2}, \frac{a_i}{2}\}$. Comparing the diversity orders for single with the multihop transmissions, the performance scaling with N can be clearly observed. Thus, the use of multiple relays enhances the OWC performance mitigating the effect of pointing errors and path loss due to fog.

C. ABER

The ABER for a variety of binary and non-binary modulation schemes can be written using the CDF of SNR (γ) [48], Eq. (40)] as:

$$\bar{P}_e = \frac{q^p}{2\Gamma(p)} \int_0^\infty \gamma^{p-1} \exp(-q\gamma) F_{\gamma_N}^{\mathrm{LR}}(\gamma) d\gamma \tag{19}$$

Substituting (10) in (19), applying the definition of Meijer's G-function, and using $\int_0^\infty \gamma^{\frac{2p+a_i+u}{2}-1} \exp(-q\gamma)d\gamma = q^{-(\frac{2p+a_i+u}{2})}\Gamma(\frac{2p+a_i+u}{2})$, we get the ABER for long-range OWC system for the single hop

$$\bar{P}_{e,i}^{\mathrm{LR}} = \frac{1}{2\Gamma(p)} \frac{a_i^{a_i} z_i^{k_i} \rho_i^2 \exp\left(\frac{-s_i^2}{2\sigma_i^2}\right)}{(A_i\sqrt{q\bar{\gamma}_i})^{a_i} \beta(a_i, b_i)(b_i-1)^{a_i}} \sum_{j=0}^\infty \frac{1}{j!} \left(\frac{s_i^2\, w_{z_{\mathrm{eq_i}}}^2}{8\sigma_i^4}\right)^j H_{3+j+k_i,4+j+k_i}^{3,2+j+k_i}\left[U_i V_i \middle| \frac{A_i\sqrt{q\bar{\gamma}_i}}{B_i}\right] \tag{20}$$

where $U_i = \{(1,1), \{(1-\rho_i^2+a_i, 1)\}_0^{j+1}, \{(1-z_i+a_i, 1)\}_1^{k_i}, (1+a_i, 1)\}$ and $V_i = \{(a_i+b_i, 1), (a_i, 1), (p+\frac{a_i}{2}, \frac{1}{2})\{(a_i-\rho_i^2, 1)\}_0^{j+1}, \{(a_i-z_i, 1)\}_1^{k_i}\}$.

Similarly, substituting (14) in (19) with $\int_0^\infty \gamma^{p-u-1}\exp(-q\gamma)d\gamma = q^{-p+u}\Gamma(p-u)$, we get the ABER for long-range OWC system for multihop systen

$$\bar{P}_{e,N}^{\mathrm{LR}} = \frac{1}{2\Gamma(p)} \prod_{i=1}^N \frac{\psi_i a_i^{a_i} z_i^{k_i} \rho_i^2 \exp\left(\frac{-s_i^2}{2\sigma_i^2}\right)}{NB_i^{a_i}\beta(a_i, b_i)(b_i-1)^{a_i}} \sum_{j=0}^\infty \frac{1}{j!} \left(\frac{s_i^2\, w_{z_{\mathrm{eq_i}}}^2}{8\sigma_i^4}\right)^j H_{4+j+k_i,3+j+k_i}^{2+j+k_i,3}\left[\begin{matrix} U_N \\ V_N \end{matrix} \middle| \prod_{i=1}^N \left(\frac{B_i}{A_i\sqrt{\bar{\gamma}_i}}\right)^{2\frac{\phi_i}{N}} \frac{1}{q}\right] \tag{21}$$

where $U_N = \{(1,1), (1-p, 1), (1-b_i, 2\frac{\phi_i}{N}), \{(1+\rho_i^2, 2\frac{\phi_i}{N})\}_0^{j+1}, \{(1+z_i, 2\frac{\phi_i}{N})\}_1^{k_i}\}$ and $V_N = \{\{(\rho_i^2, 2\frac{\phi_i}{N})\}_0^{j+1}, \{(z_i, 2\frac{\phi_i}{N})\}_1^{k_i}, (a_i, 2\frac{\phi_i}{N}), (0,1)\}$.

Note that an asymptotic expression for the ABER can be similarly derived by applying the series expansion of single-variate Fox's H function [47], Eq. 1.8.4], as done for the OP.

IV. Short-Range OWC System

The atmospheric turbulence is the effect of change in the refractive index of the medium when the optical signal is transmitted. It is customary to neglect the atmospheric turbulence for short-range communications, especially in foggy weather conditions [39]. Moreover, the derived statistical results (in Section III) for the long-range system consist of Mellin-Bernes integral. A simpler mathematical representation for the short-range system might be possible due to the absence of the atmospheric turbulence channel component. Although short-range performance can be obtained from the long-range performance by invoking $a_i \to \infty$ and $b_i \to \infty$ in the corresponding analytical expressions, computing the limit on Mellin-Bernes integral is not trivial, necessitating independent analysis for the short-range system. In this section, we analyze the performance of short-range OWC system over the foggy channel with generalized pointing errors.

A. PDF and CDF of SNR

Lemma 2: The PDF and CDF of SNR for a single-hop OWC system over fog-induced fading with non-zero boresight pointing errors are given as:

$$f_{\gamma_i}^{\mathrm{SR}}(\gamma) = \frac{{z_i}^{k_i} {\rho_i}^2 \exp\left(\frac{-{s_i}^2}{2{\sigma_i}^2}\right)}{2\Gamma(k_i) A_i^{\rho_i^2}\sqrt{\gamma\bar{\gamma}_i}} \sum_{j=0}^\infty \frac{1}{(j!)^2} \left(\frac{{s_i}^2\, w_{z_{\mathrm{eq_i}}}^2}{8\sigma_i^4}\right)^j \left(\sqrt{\frac{\gamma}{\bar{\gamma}_i}}\right)^{\rho_i^2-1} \sum_{n=0}^j \binom{j}{n} (-1)^n \left(\ln\frac{A_i\sqrt{\bar{\gamma}_i}}{\sqrt{\gamma}}\right)^{j-n} m^{-n-k_i}\left[\Gamma(n+k_i) - \Gamma\left(n+k_i, m_i \ln\frac{A_i\sqrt{\bar{\gamma}_i}}{\sqrt{\gamma}}\right)\right] \tag{22}$$

$$F_{\gamma_i}^{\mathrm{SR}}(\gamma) = \frac{{z_i}^{k_i} {\rho_i}^2 \exp\left(\frac{-s_i^2}{2\sigma_i^2}\right)}{\Gamma(k_i)} \sum_{j=0}^\infty \frac{1}{(j!)^2} \left(\frac{s_i^2\, w_{z_{\mathrm{eq_i}}}^2}{8\sigma_i^4}\right)^j \sum_{n=0}^j \binom{j}{n} \frac{(-1)^n}{m_i^{j+k_i+1}} \left[\frac{\Gamma(n+k_i)\Gamma\left(1+j-n, \rho_i^2 \ln\frac{A_i\sqrt{\bar{\gamma}_i}}{\sqrt{\gamma}}\right)}{\left(\frac{\rho_i^2}{m_i}\right)^{j-n+1}} - \frac{(n+k_i-1)!\Gamma\left(1+j-n+l, \left(\frac{\rho_i^2}{m_i}+1\right) m_i \ln\frac{A_i\sqrt{\bar{\gamma}_i}}{\sqrt{\gamma}}\right)}{\left(\frac{\rho_i^2}{m_i}+1\right)^{j-n+l+1}}\right] \tag{23}$$

where $0 \leq \gamma \leq A_i^2\bar{\gamma}_i$.

Proof: See Appendix C. ■

It can be seen that (22) and (23) generalizes the analysis presented in [36] for zero boresight pointing errors. Thus, substituting $s = 0$ in (22) and (23), we can get PDF and CDF for the zero boresight OWC system, respectively.

Similar to the previous subsection, We use (11) to develop statistical results for the short-range multihop transmissions.

Theorem 2: The PDF and CDF of SNR for a multihop OWC system over fog-induced fading with non-zero boresight pointing errors are given as:

$$f_{\gamma_N}^{\mathrm{SR}}(\gamma) = \prod_{i=1}^N \frac{\psi_i z_i^{k_i} \rho_i^2 \exp\left(\frac{-s_i^2}{2\sigma_i^2}\right)}{N\gamma m_i^{j+k_i+1}\Gamma(k_i)} \sum_{j=0}^\infty \frac{1}{(j!)^2}$$

$$\times \left(\frac{s_i^2\, w_{z_{\mathrm{eq_i}}}^2}{8\sigma_i^4}\right)^j \sum_{n=0}^{j}\binom{j}{n}(-1)^n \left[\Gamma(n+k_i)\Gamma(1+j-n)\right.$$

$$\times H_{n-j-1,n-j-1}^{n-j-1,0}\left[\begin{matrix}\{(1+\frac{\rho_i^2}{m_i},\frac{2\phi_i}{m_i N})\}_{n=0,j=0}^{n-j-1}\\ \{(\frac{\rho_i^2}{m_i},\frac{2\phi_i}{m_i N})\}_{n=0,j=0}^{n-j-1}\end{matrix}\middle|\prod_{i=1}^{N}\frac{\gamma}{(A_i^2\bar{\gamma}_i)^{\frac{\phi_i}{N}}}\right]$$

$$-(n+k-1)!$$

$$\times \sum_{l=0}^{n+k-1}\frac{1}{l!}\Gamma(1+j-n+l)H_{n-j-l-1,n-j-l-1}^{n-j-l-1,0}$$

$$\left.\left[\begin{matrix}\{(2+\frac{\rho_i^2}{m_i},\frac{2\phi_i}{m_i N})\}_{n=0,j=0,l=0}^{n-j-l-1}\\ \{(1+\frac{\rho_i^2}{m_i},\frac{2\phi_i}{m_i N})\}_{n=0,j=0,l=0}^{n-j-l-1}\end{matrix}\middle|\prod_{i=1}^{N}\frac{\gamma}{(A_i^2\bar{\gamma}_i)^{\frac{\phi_i}{N}}}\right]\right] \tag{24}$$

$$F_{\gamma_N}^{\mathrm{SR}}(\gamma)=\prod_{i=1}^{N}\frac{\psi_i z_i^{k_i}\rho_i^2\exp\left(\frac{-s_i^2}{2\sigma_i^2}\right)}{N m_i^{j+k_i+1}\Gamma(k_i)}\sum_{j=0}^{\infty}\frac{1}{(j!)^2}$$

$$\times\left(\frac{s_i^2\, w_{z_{\mathrm{eq_i}}}^2}{8\sigma_i^4}\right)^j\sum_{n=0}^{j}\binom{j}{n}(-1)^n\left[\Gamma(n+k_i)\Gamma(1+j-n)\right.$$

$$\times H_{n-j,n-j}^{n-j-1,1}\left[\begin{matrix}(1,1),\{(1+\frac{\rho_i^2}{m_i},\frac{2\phi_i}{m_i N})\}_{n=0,j=0}^{n-j-1}\\ \{(\frac{\rho_i^2}{m_i},\frac{2\phi_i}{m_i N})\}_{n=0,j=0}^{n-j-1},(0,1)\end{matrix}\right.$$

$$\times\left|\prod_{i=1}^{N}\frac{\gamma}{(A_i^2\bar{\gamma}_i)^{\frac{\phi_i}{N}}}\right]$$

$$-(n+k-1)!\sum_{l=0}^{n+k-1}\frac{1}{l!}\Gamma(1+j-n+l)H_{n-j-l,n-j-l}^{n-j-l-1,1}$$

$$\left.\left[\begin{matrix}(1,1),\{(2+\frac{\rho_i^2}{m_i},\frac{2\phi_i}{m_i N})\}_{n=0,j=0,l=0}^{n-j-l-1}\\ \{(1+\frac{\rho_i^2}{m_i},\frac{2\phi_i}{m_i N})\}_{n=0,j=0,l=0}^{n-j-l-1},(0,1)\end{matrix}\middle|\prod_{i=1}^{N}\frac{\gamma}{(A_i^2\bar{\gamma}_i)^{\frac{\phi_i}{N}}}\right]\right] \tag{25}$$

(26) shown at the bottom of this page, where $\mathcal{A}_{i'}=\mathcal{A}_{j'}=\{1,\{1+\frac{\rho_i^2}{m_i}\}_{n=0,j=0}^{n-j-1}\}$, $\mathcal{B}_{i'}=\mathcal{B}_{j'}=\{1,\{\frac{2\phi_i}{m_i N}\}_{n=0,j=0}^{n-j-1}\}$, $\mathcal{C}_{i'}=\mathcal{C}_{j'}=\{\{\frac{\rho_i^2}{m_i}\}_{n=0,j=0}^{n-j-1},0\}$, $\mathcal{D}_{i'}=\mathcal{D}_{j'}=\{\{\frac{2\phi_i}{m_i N}\}_{n=0,j=0}^{n-j-1},1\}$, $\mathcal{P}_{i'}=\mathcal{P}_{j'}=\{1,\{2+\frac{\rho_i^2}{m_i}\}_{n=0,j=0,l=0}^{n-j-l-1}\}$, $\mathcal{Q}_{i'}=\mathcal{Q}_{j'}=\{1,\{\frac{2\phi_i}{m_i N}\}_{n=0,j=0,l=0}^{n-j-l-1}\}$, $\mathcal{R}_{i'}=\mathcal{R}_{j'}=\{\{1+\frac{\rho_i^2}{m_i}\}_{n=0,j=0,l=0}^{n-j-l-1},0\}$, and $\mathcal{S}_{i'}=\mathcal{S}_{j'}=\{\{\frac{2\phi_i}{m_i N}\}_{n=0,j=0,l=0}^{n-j-l-1},1\}$.

Proof: See Appendix D. ∎

B. Outage Probability

Substituting (23) in (16), we can get an exact OP for the single-hop transmissions. Further, we apply $\frac{\Gamma(s,x)}{x^{s-1}\exp(-x)}\to 1$ as $x\to\infty$ in (23) to find the asymptotic expression of the OP at high SNR

$$OP_i^{\mathrm{SR},\infty}=\frac{{z_i}^{k_i}{\rho_i}^2\exp\left(\frac{-s_i^2}{2\sigma_i^2}\right)}{\Gamma(k_i)}\sum_{j=0}^{\infty}\frac{1}{(j!)^2}\left(\frac{s_i^2\, w_{z_{\mathrm{eq_i}}}^2}{8\sigma_i^4}\right)^j$$

$$\times\sum_{n=0}^{j}\binom{j}{n}\frac{(-1)^n\Gamma(n+k_i)}{m_i^{j+k_i+1}}$$

$$\times\left[\frac{\left(\rho_i^2\ln\frac{A_i\sqrt{\bar{\gamma}_i}}{\sqrt{\gamma_{\mathrm{th}}}}\right)^{j-n}\left(\frac{A_i\sqrt{\bar{\gamma}_i}}{\sqrt{\gamma_{\mathrm{th}}}}\right)^{-\rho_i^2}}{\left(\frac{\rho_i^2}{m_i}\right)^{j-n+1}}\right.$$

$$\left.-\frac{\left(z_i\ln\frac{A_i\sqrt{\bar{\gamma}_i}}{\sqrt{\gamma_{\mathrm{th}}}}\right)^{j-n+l}\left(\frac{A_i\sqrt{\bar{\gamma}_i}}{\sqrt{\gamma_{\mathrm{th}}}}\right)^{-z_i}}{\left(\frac{z_i}{m_i}\right)^{j-n+l+1}}\right] \tag{27}$$

Compiling the exponent of $\bar{\gamma}_i$, the diversity order for the single-hop transmission is $DO_i^{\mathrm{SR}}=\min\{\frac{z_i}{2},\frac{\rho_i^2}{2}\}$. It can be seen that the diversity order for the single-hop OWC system is exactly the same as that of the OWC, with zero boresight pointing errors [49]. Thus, there is no impact of non-zero boresight parameter $s\neq 0$ on the diversity order of the system.

Similarly, we can substitute the CDF (as given in (25)) of multihop link in (16) to get the OP for the short-range multihop transmissions. We can apply the series expansion of single-variate Fox's H function [47], Eq. 1.8.4] to derive the asymptotic expression for the OP in high SNR regime $\bar{\gamma}_i\to\infty,\forall i$ in (26).

Using (26), we can find the diversity order as $DO_N^{\mathrm{LR}}=\sum_i^N\min\{\frac{z_i}{2},\frac{\rho_i^2}{2}\}$, which is a special case for the long-range multihop communications. Thus, the use of multiple relays provides the capability to mitigate the effect of pointing errors and signal attenuation due to the fog.

$$OP_N^{\mathrm{SR},\infty}=\prod_{i=1}^{N}\frac{\psi_i z_i^{k_i}\rho_i^2\exp\left(\frac{-s_i^2}{2\sigma_i^2}\right)}{N m_i^{j+k_i+1}\Gamma(k_i)}(A_i^2\bar{\gamma}_i)^{u\frac{\phi_i}{N}}\sum_{j=0}^{\infty}\frac{1}{(j!)^2}\left(\frac{s_i^2\, w_{z_{\mathrm{eq_i}}}^2}{8\sigma_i^4}\right)^j\sum_{n=0}^{j}\binom{j}{n}(-1)^n\Gamma(n+k_i)\left[\Gamma(1+j-n)\sum_{j'=1}^{n-j-1}\right.$$

$$\left(\prod_{i=1}^{N}\frac{\gamma_{\mathrm{th}}}{(A_i^2\bar{\gamma}_i)^{\frac{\phi_i}{N}}}\right)^{\frac{\mathcal{C}_{j'}}{\mathcal{D}_{j'}}}\frac{1}{\mathcal{D}_{j'}}\frac{\prod_{i'=1,i'\neq j'}^{n-j-1}\Gamma\left(\mathcal{C}_{i'}-\mathcal{C}_{j'}\frac{\mathcal{D}_{i'}}{\mathcal{D}_{j'}}\right)\Gamma\left(\frac{\mathcal{C}_{j'}}{\mathcal{D}_{j'}}\right)}{\prod_{i'=2}^{n-j}\Gamma\left(\mathcal{A}_{i'}-\mathcal{C}_{j'}\frac{\mathcal{B}_{i'}}{\mathcal{D}_{j'}}\right)\Gamma\left(1+\frac{\mathcal{C}_{j'}}{\mathcal{D}_{j'}}\right)}-\sum_{l=0}^{n+k-1}\frac{1}{l!}\Gamma(1+j-n+l)\sum_{j'=1}^{n-j-l-1}\left(\prod_{i=1}^{N}\frac{\gamma_{\mathrm{th}}}{(A_i^2\bar{\gamma}_i)^{\frac{\phi_i}{N}}}\right)^{\frac{\mathcal{R}_{j'}}{\mathcal{S}_{j'}}}$$

$$\left.\frac{1}{\mathcal{S}_{j'}}\frac{\prod_{i'=1,i'\neq j'}^{n-j-l-1}\Gamma\left(\mathcal{R}_{i'}-\mathcal{R}_{j'}\frac{\mathcal{S}_{i'}}{\mathcal{S}_{j'}}\right)\Gamma\left(\frac{\mathcal{R}_{j'}}{\mathcal{S}_{j'}}\right)}{\prod_{i'=2}^{n-j-l}\Gamma\left(\mathcal{P}_{i'}-\mathcal{R}_{j'}\frac{\mathcal{Q}_{i'}}{\mathcal{S}_{j'}}\right)\Gamma\left(1+\frac{\mathcal{R}_{j'}}{\mathcal{S}_{j'}}\right)}\right] \tag{26}$$

C. ABER

The ABER for a variety of binary modulation schemes can be written using the PDF of SNR as

$$\bar{P}_e = p\int_0^\infty Q(\sqrt{q\gamma}) f_{\gamma_i}(\gamma)d\gamma \tag{28}$$

where the constants p, q, provide flexibility to design various modulation schemes. Using (22) in (28) with the series expansion $\Gamma(a,t) \triangleq (a-1)!e^{-t}\sum_{m=0}^{a-1}\frac{t^m}{m!}$, we get

$$\bar{P}_{e,i}^{\mathrm{SR}} = p\int_0^{A_i^2\bar{\gamma}_i} Q(\sqrt{q\gamma})\frac{z_i^{k_i}\rho_i^2\exp\left(\frac{-s_i^2}{2\sigma_i^2}\right)}{2\Gamma(k_i)A_0^{\rho_i^2}\sqrt{\gamma\bar{\gamma}_i}}\sum_{j=0}^{\infty}\frac{1}{(j!)^2} \left(\frac{s_i^2\, w_{z_{\mathrm{eq_i}}}^2}{8\sigma_i^4}\right)^j\left(\sqrt{\frac{\gamma}{\bar{\gamma}_i}}\right)^{\rho_i^2-1}\sum_{n=0}^{j}(jn)(-1)^n \left(\ln\frac{A_i\sqrt{\bar{\gamma}_i}}{\sqrt{\gamma}}\right)^{j-n} m_i^{-n-k_i}\Bigg[\Gamma(n+k_i)-(n+k_i-1)! \left(\frac{A_i\sqrt{\bar{\gamma}_i}}{\sqrt{\gamma}}\right)^{-m_i}\sum_{l=0}^{n+k_i-1}\frac{\left(m_i\ln\frac{A_i\sqrt{\bar{\gamma}_i}}{\sqrt{\gamma}}\right)^l}{l!}\Bigg]d\gamma \tag{29}$$

Applying $Q(\sqrt{q\gamma}) = G_{1,2}^{2,0}\left[{}^{\ 1}_{0,\frac{1}{2}}\middle|\frac{q}{2}\gamma\right] = \frac{1}{2\pi i}\int_L\frac{\Gamma(-u)\Gamma(\frac{1}{2}-u)}{\Gamma(1-u)}(\frac{q}{2}\gamma)^u$ and substituting $\ln\frac{A_i\sqrt{\bar{\gamma}_i}}{\sqrt{\gamma}} = t$ and $d\gamma = -2\,A_i^2\bar{\gamma}_i\exp(-2t)dt$ in (29), we solve the integrals $\int_0^\infty t^{j-n}\exp[-(\rho_i^2+u)t]dt = \Gamma(1+j-n)(\frac{\Gamma(\rho_i^2+2\,u)}{\Gamma(1+\rho_i^2+2\,u)})^{n-j-1}$ and $\int_0^\infty t^{j-n+l}\exp[-(z_i+u)t]dt = \Gamma(1+j-n+l)(\frac{\Gamma(z_i+2\,u)}{\Gamma(1+z_i+2\,u)})^{n-j-l-1}$. Using these integral, we apply the definition of Fox's H-function in (29) to get a analytical expression for the ABER for the single-hop OWC system as:

$$\bar{P}_{e,i}^{\mathrm{SR}} = \frac{z_i^{k_i}\rho_i^2\exp\left(\frac{-s_i^2}{2\sigma_i^2}\right)}{2\Gamma(k_i)A_0^{\rho_i^2}\sqrt{\gamma\bar{\gamma}_i}}\sum_{j=0}^{\infty}\frac{1}{(j!)^2}\left(\frac{s_i^2\, w_{z_{\mathrm{eq_i}}}^2}{8\sigma_i^4}\right)^j \left(\sqrt{\frac{\gamma}{\bar{\gamma}_i}}\right)^{\rho_i^2-1}\sum_{n=0}^{j}\binom{j}{n}(-1)^n\left(\ln\frac{A_i\sqrt{\bar{\gamma}_i}}{\sqrt{\gamma}}\right)^{j-n}m_i^{-n-k_i} \Bigg[\Gamma(n+k_i)H_{n-j+1,n-j}^{n-j-1,2}\left[\begin{matrix}(1,1),(\frac{1}{2},1),\{(1+\rho_i^2,2)\}^{n-j-1}\\ \{(\rho_i^2,2)\}^{n-j-1},(0,1)\end{matrix}\middle|\frac{2}{qA_i^2\bar{\gamma}_i}\right]-(n+k_i-1)! \sum_{l=0}^{n+k_i-1}\frac{\Gamma(1+j-n+l)}{l!}H_{n-j-l+1,n-j-l}^{n-j-l-1,2} \left[\begin{matrix}(1,1),(\frac{1}{2},1),\{(1+z_i,2)\}^{n-j-l-1}\\ \{(z_i,2)\}^{n-j-l-1},(0,1)\end{matrix}\middle|\frac{2}{qA_i^2\bar{\gamma}_i}\right]\Bigg] \tag{30}$$

To derive the ABER for the multihop system, we substitute (24) in (28), apply $Q(\sqrt{q\gamma}) = G_{1,2}^{2,0}\left[{}^{\ 1}_{0,\frac{1}{2}}\middle|\frac{q}{2}\gamma\right] = \frac{1}{2\pi\jmath}\int_{\mathcal{L}}\frac{\Gamma(-u_1)\Gamma(\frac{1}{2}-u_1)}{\Gamma(1-u_1)}(\frac{q}{2}\gamma)^{u_1}$ and definition of Fox's H-function, we get

$$\bar{P}_{e,N}^{\mathrm{SR}} = p\int_0^{A_i^2\bar{\gamma}_i}\frac{1}{2\pi\jmath}\int_{\mathcal{L}}\frac{\Gamma(-u_1)\Gamma(\frac{1}{2}-u_1)}{\Gamma(1-u_1)}\left(\frac{q}{2}\gamma\right)^{u_1}\prod_{i=1}^{N} \frac{\psi_i z_i^{k_i}\rho_i^2\exp\left(\frac{-s_i^2}{2\sigma_i^2}\right)}{N\gamma m_i^{j+k_i+1}\Gamma(k_i)}\sum_{j=0}^{\infty}\frac{1}{(j!)^2}\left(\frac{s_i^2\, w_{z_{\mathrm{eq_i}}}^2}{8\sigma_i^4}\right)^j \sum_{n=0}^{j}\binom{j}{n}(-1)^n[\Gamma(n+k_i)\Gamma(1+j-n) \frac{1}{2\pi\jmath}\int_{\mathcal{L}}\left(\frac{\Gamma\left(\frac{\rho_i^2}{m_i}+\frac{2\phi_i}{m_iN}u_2\right)}{\Gamma\left(1+\frac{\rho_i^2}{m_i}+\frac{2\phi_i}{m_iN}u_2\right)}\right)^{n-j-1}\left(\frac{\gamma}{(A_i^2\bar{\gamma}_i)^{\frac{\phi_i}{N}}}\right)^{-u_2} -(n+k-1)!\sum_{l=0}^{n+k-1}\frac{1}{l!}\Gamma(1+j-n+l) \frac{1}{2\pi\jmath}\int_{\mathcal{L}}\left(\frac{\Gamma(1+\frac{\rho_i^2}{m_i}+\frac{2\phi_i}{m_iN}u_2)}{\Gamma(2+\frac{\rho_i^2}{m_i}+\frac{2\phi_i}{m_iN}u_2)}\right)^{n-j-l-1}\left(\frac{\gamma}{(A_i^2\bar{\gamma}_i)^{\frac{\phi_i}{N}}}\right)^{-u_2}]d\gamma \tag{32}$$

Solving the above inner integral $\int_0^{A_i^2\bar{\gamma}_i}\gamma^{u_1-u_2-1}d\gamma = \frac{(A_i^2\bar{\gamma}_i)^{u_1-u_2}}{u_1-u_2} = \frac{\Gamma(u_1-u_2)}{\Gamma(1+u_1-u_2)}$ and substituting $u_2\to -u_2$, and applying the definition of bivariate Fox's H-function [50], we get the ABER in (31), shown at the bottom of this page

$$\bar{P}_{e,N}^{\mathrm{SR}} = p\prod_{i=1}^{N}\frac{\psi_i z_i^{k_i}\rho_i^2\exp\left(\frac{-s_i^2}{2\sigma_i^2}\right)}{Nm_i^{j+k_i+1}\Gamma(k_i)}\sum_{j=0}^{\infty}\frac{1}{(j!)^2}\left(\frac{s_i^2\, w_{z_{\mathrm{eq_i}}}^2}{8\sigma_i^4}\right)^j\sum_{n=0}^{j}\binom{j}{n}(-1)^n\Bigg[\Gamma(n+k_i)\Gamma(1+j-n)H_{1,1:1,2;n-j-1,n-j-1}^{0,1:2,0;n-j-1,0} \left[\begin{matrix}(1;1,1):(1,1);\{(1+\frac{\rho_i^2}{m_i},\frac{2\phi_i}{m_iN})\}_{n=0,j=0}^{n-j-1}\\ (0;1,1):(0,1),(\frac{1}{2},1);\{(\frac{\rho_i^2}{m_i},\frac{2\phi_i}{m_iN})\}_{n=0,j=0}^{n-j-1}\end{matrix}\middle|\prod_{i=1}^{N}\frac{A_i^2\bar{\gamma}_iq}{2},\prod_{i=1}^{N}(A_i^2\bar{\gamma}_i)^{1-\frac{\phi_i}{N}}\right]-(n+k-1)!\sum_{l=0}^{n+k-1}\frac{1}{l!}\Gamma(1+j-n+l) H_{1,1:1,2;n-j-l-1,n-j-l-1}^{0,1:2,0;n-j-l-1,0}\left[\begin{matrix}(1;1,1):(1,1);\{(2+\frac{\rho_i^2}{m_i},\frac{2\phi_i}{m_iN})\}_{n=0,j=0,l=0}^{n-j-l-1}\\ (0;1,1):(0,1),(\frac{1}{2},1);\{(1+\frac{\rho_i^2}{m_i},\frac{2\phi_i}{m_iN})\}_{n=0,j=0,l=0}^{n-j-l-1}\end{matrix}\middle|\prod_{i=1}^{N}\frac{A_i^2\bar{\gamma}_iq}{2},\prod_{i=1}^{N}(A_i^2\bar{\gamma}_i)^{1-\frac{\phi_i}{N}}\right]\Bigg] \tag{31}$$

TABLE III
SIMULATION PARAMETERS

Transmitted power	P_t	0 to 40 dBm
Responsitivity	R	0.4 A/W
AWGN variance	σ_w^2	10^{-14} A^2/GHz
Long-range distance	d_{LR}	1500 m
Short-range distance	d_{SR}	500 m
Threshold SNR	γ_{th}	6 dB
Shape parameter of fog	k	{2.32, 5.49, 6.00}
Scale parameter of fog	β	{13.12, 12.06, 23.00}
Aperture diameter	$D = 2a_r$	10 cm
Normalized beam-width	w_z/a_r	{3, 6}
Jitter standard deviation	σ_s	{5-20} cm
Horizontal and vertical displacement	μ_{x_i}, μ_{y_i}	{0.1, 0.1} m
Wavelength	λ	1550 nm
Turbulence parameters	a_i,b_i	{4.5916, 2.3378, 1.4321}, {7.0941, 4.5323, 3.4948}

V. SIMULATION AND NUMERICAL ANALYSIS

In this section, we investigate the performance of multihop OWC system over atmospheric turbulence and fog with generalized pointing errors using both numerical and Monte Carlo (MC) simulation (averaged over 10^7 channel realizations) approaches. We use 20 terms of the series expansion to numerically evaluate the derived expressions. We consider two simulation scenarios: short-range (link distance limited to 500 m) communication over fog with generalized pointing errors and long-range (link distance above 1000 m) communication over atmospheric turbulence and fog with generalized pointing errors. To ensure that each hop of long-range is higher than the short range system, we have limited the short-range to 500 m. We validate our derived analytical expressions (depicted with corresponding equation numbers) with numerical and simulation results. We demonstrate the significance of multihop relaying as compared with the single-hop transmission for various link distances and channel impairments (turbulence, fog, and pointing errors). We list the simulation parameters in Table III. The fixed gain relaying factor is obtained using statistics of the received signal of the previous hop $C_i = (\mathbb{E}(1+\gamma_i)^{-1})^{-1}$ with $C_0 = 1$ and $\mathbb{E}$ denotes the expectation operator. We denote the acronyms used in the legend of figures as SH to single-hop, MH to multihop, SR to short-range, and LR to long-range.

In Fig. 2, we demonstrate the convergence of the PDF of the non-zero boresight pointing errors (as expressed using infinite series in (8)) to the exact within a few terms. The figure shows that the error between the exact PDF and its series representation is indistinguishable when the number of terms is more than 10. In all the following plots, we use 20 terms to reduce the error in computation.

We illustrate the impact of probabilistic attenuation compared with the deterministic attenuation in a typical foggy condition, as shown in Fig. 3. There is a gap of around 3 dB when the average SNR using probabilistic path loss is compared with the deterministic path loss for the visibility range of 800 m. The gap becomes higher when the visibility range is reduced to 600 m. Thus, the probabilistic path loss model can provide a realistic estimate of the performance of OWC over foggy conditions.

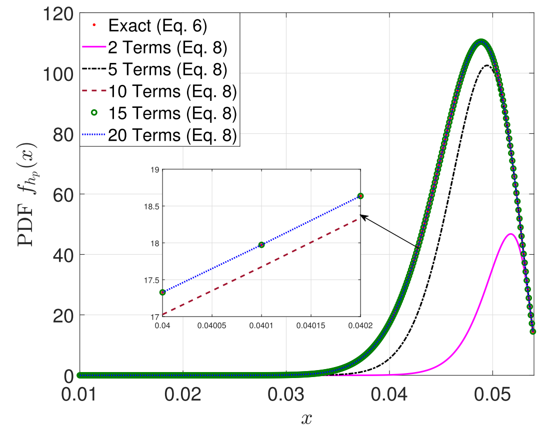

Fig. 2. Convergence of the PDF for non-zero boresight pointing errors.

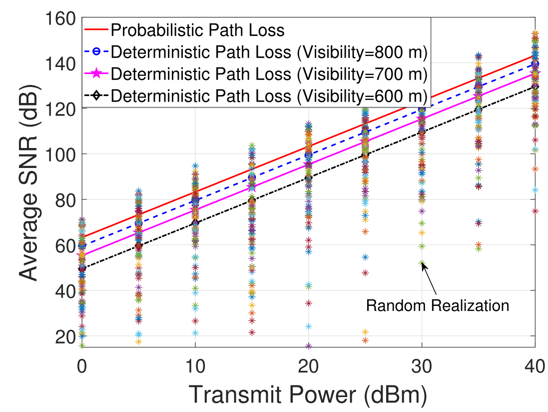

Fig. 3. Average and random realizations of the SNR with probabilistic and deterministic path loss.

Further, random realizations in Fig. 3 shows a huge variation in the channel fading under foggy weather.

In Fig. 4, we demonstrate the significance of multihop relaying for the OWC system under the combined effect of atmospheric turbulence, pointing errors, and random fog. We consider different atmospheric turbulence conditions (weak, moderate, and strong) with light fog and compare the OP with the single-hop, two hops, and three hops OWC system, as depicted in Fig. 4(a). The impact of turbulence intensity is not significant if the performance degradation with strong turbulence is compared with the weak one. Further, multihop relaying with $N = 3$ significantly improves the OP.

We take two scenarios where the inverse correlation between turbulence and fog has been adopted by considering strong turbulence with light fog and moderate turbulence in the high-density moderate fog condition. We plot the ABER performance of the direct link, two hop, and three hop OWC system, as shown in Fig. 4(b). The ABER performance is extremely poor for both moderate and light foggy conditions with the direct transmission for the link distance of 1500 m. However, the ABER is significantly improved when the multihop relaying is employed. A dual-hop transmission is sufficient to achieve an acceptable ABER of 10^{-3} at a transmit power in light fog, where

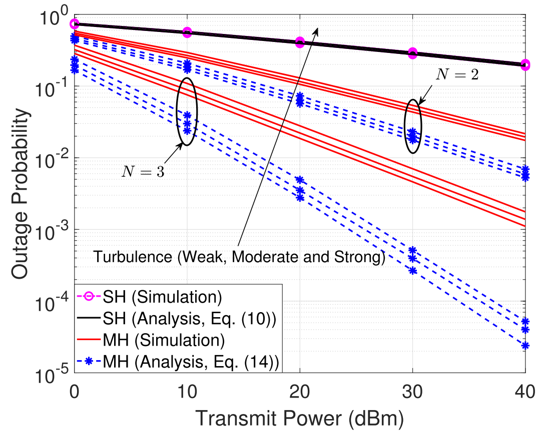

(a) OP for different turbulence conditions over light fog.

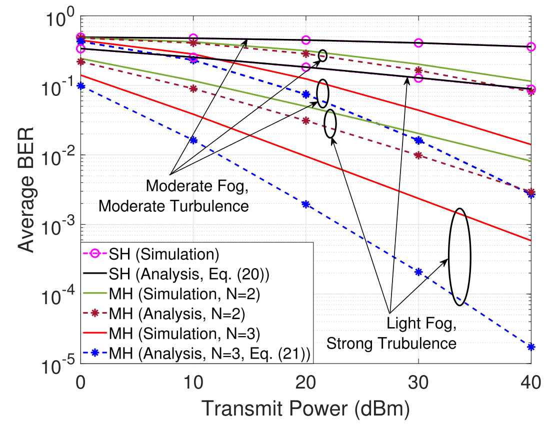

(b) ABER over different fog and turbulence conditions.

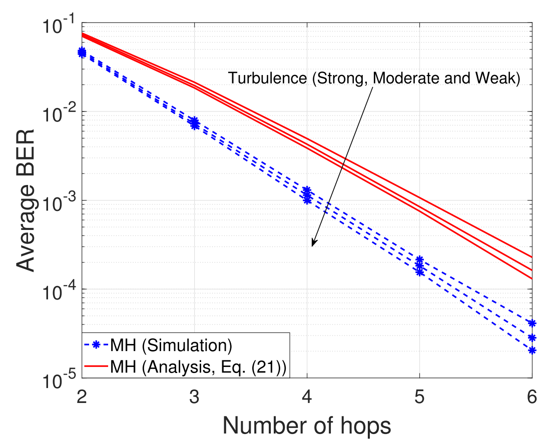

(c) ABER over light fog and different turbulence conditions at transmit power $P_i = 60\text{dBm}$ and total link distance $d_i = 3$ km.

Fig. 4. Performance for long-range OWC systems over random fog, atmospheric turbulence with pointing error parameters $\frac{w_z}{a_r} = 6$ and $\sigma_s = 5\,\text{cm}$.

a few additional hops are required to achieve the same performance in moderate fog conditions. In Fig. 4(c), we describe the impact of the number of hops on the ABER performance for different turbulence conditions (weak, moderate, and strong). The figure shows the performance scaling with the number of hops achieving an acceptable ABER of 10^{-3} within 5 hops at a 10 dBm transmit power.

In Fig. 5, we demonstrate the performance of OWC for short-range communication under the combined effect of random fog and pointing errors with negligible atmospheric turbulence. We plot the OP of the OWC system for short-range communication, as depicted in Fig. 5(a). We demonstrate the impact of fog density and pointing errors on the performance of multihop OWC system by considering a single hop (direct link), two hops, and three hops scenarios. It can be seen from Fig. 5(a) that there is a significant improvement in the OP performance with an increase in the number of hops. The figure shows that single hop transmission is not useful even at a transmit power of 40 dBm with OP more than 10^{-2}. The dual-hop and triple-hop transmissions attain an acceptable OP in the range of 10^{-4} and 10^{-6}, respectively. We can also observe the impact of pointing errors parameters ($\frac{w_z}{a_r} = \{3, 6\}$ and $\sigma_s = \{5 - 20\}\,\text{cm}$) on the OP. In Fig. 5(b), we plot the OP versus the number of hops at a transmit power 10dBm to show the scaling of performance considering light and moderate fog with different pointing errors parameters ($\frac{w_z}{a_r} = \{3, 6\}$ and $\sigma_s = \{5 - 20\}\,\text{cm}$). The figure shows that the OP improves as we increase the number of hops. The number of hops required is less in the light foggy condition than the moderate fog to achieve an acceptable OP of 10^{-3}.

In Fig. 5(c), we illustrate the ABER performance for short-range OWC system over the foggy channel with pointing errors. We demonstrate the effect of multihop relaying on the ABER performance for moderate foggy conditions and pointing errors ($\frac{w_z}{a_r} = 6$ and $\sigma_s = 5\,\text{cm}$) at two link distances ($\{d = 0.8, 1\}\,\text{km}$). The figure shows that the ABER is too high for practical practices in a single hop transmission for moderate fog conditions. However, the use of two relays (i.e., $N = 3$ hops) significantly improves the ABER performance of the OWC system.

In Figs. 4 and 5, we validate the derived analytical expressions with simulations for both single and multihop systems. It can be seen that there is an excellent match between analytical and simulation results for the single-hop system. However,

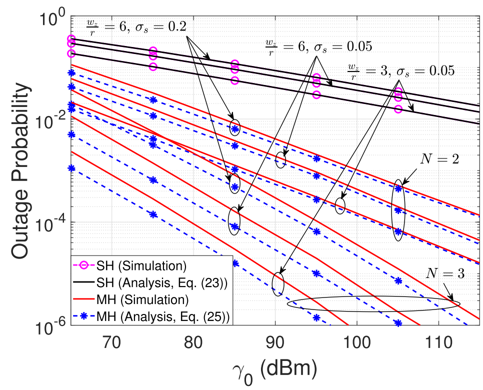

(a) OP analysis over light fog with different pointing errors conditions with total link distance $d_i = 500$ m.

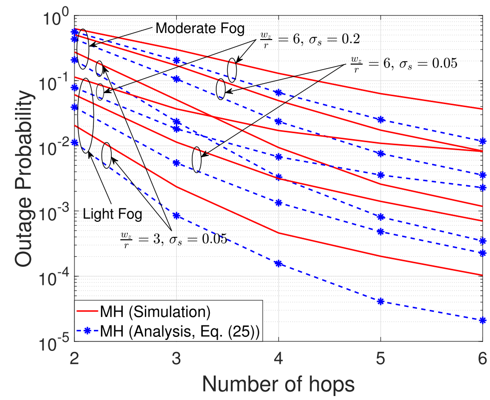

(b) OP analysis over light fog and moderate fog with different pointing errors conditions at transmit power $P_i = -5$dBm and total link distance $d_i = 500$ m.

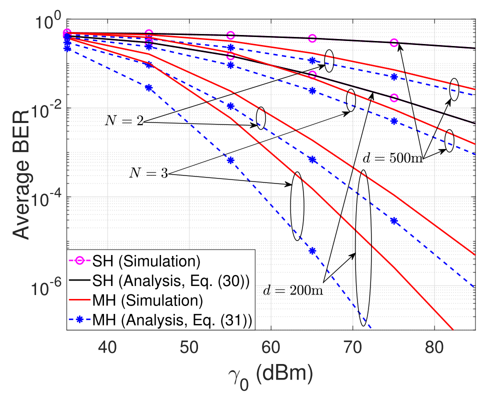

(c) ABER over moderate fog with pointing error parameters $\frac{w_z}{a_r} = 6$ and $\sigma_s = 5$ cm.

Fig. 5. Performance for short-range OWC systems over random fog and pointing errors.

there is a gap between the derived upper bound (applying the inequality between geometric mean and harmonic mean) and Monte Carlo simulation for the multihop system. The figures show that the difference between simulations and upper bounds increases when the number of hops increases. However, it can be seen that a few hops are sufficient to achieve desirable performance. Fig. 4(a) shows that the upper bound overestimates the performance by 10dBm for $N = 2$ and 20 dBm for $N = 3$ in the case of long-range transmission, whereas the gap between analytical and simulation results for the short-range system is less (overestimated by 5dBm for $N = 2$ and 10 dBm for $N = 3$) compared with the long-range system. Further, the derived upper bound enables the development of asymptotic expressions at a high SNR, which can help adapt efficient design parameters for practical deployment scenarios.

VI. Conclusion

We analyzed the performance of a fixed-gain AF relaying based multihop OWC system over atmospheric turbulence and non-zero boresight pointing errors with fog-induced fading. We also analyzed a particular multihop system for short-range communication without considering atmospheric turbulence. We presented the OP and ABER performance for both multihop systems by deriving analytical expressions for the PDF and CDF of the end-to-end SNR. We also developed performance metrics for the single-hop system to compare with the multihop transmission. The diversity order of the considered systems is presented using asymptotic analysis in high SNR to provide better insight into the performance dependency with various channel and system parameters. We presented extensive simulation results to demonstrate the significance of multihop relaying to extend the communication range. The single-hop transmission does not provide acceptable performance for a longer link over 1500 m under foggy conditions. Further, there exists a gap between the derived upper bounds and simulation results when the number of hops increases. However, the OWC system requires a few hops only to achieve acceptable performance for a typical terrestrial communication advocating the significance of analytical bounds. A dual-hop transmission is sufficient to achieve an acceptable outage and error performance in light fog, where a few additional hops are required to achieve the same performance in moderate fog conditions.

We envision that the proposed multihop transmission considering generalized fading scenarios would be helpful to assess the deployment of the OWC system for terrestrial backhaul/fronthaul applications. Further, a quantitative comparison between energy consumption with additional relays and communication performance for the multihop transmission can be investigated as the future scope of the proposed work.

Appendix A
Lemma 1 (Long-Range and Single-Hop)

Applying the theory of product distribution, the PDF of $h_{tp_i} = h_{p_i} h_{t_i}$ can be expressed as

$$f_{h_{tp_i}}(x) = \int_0^{A_i} \frac{1}{|h_{p_i}|} f_{h_{t_i}}(x/h_{p_i}) f_{h_{p_i}}(h_{p_i}) dh_{p_i} \quad (33)$$

We use the identity $\frac{1}{(pt+1)^q} = G_{1,1}^{1,1}\left[\begin{matrix}1-q\\0\end{matrix}\middle| pt\right]$ [[51], Eq. (8.4.2.5)] in (7), we express the PDF of $\mathcal{F}$ distribution $f_{h_{t_i}}(x)$ by

$$f_{h_{t_i}}(x) = \frac{a_i^{a_i} x^{a_i-1}}{\beta(a_i,b_i)(b_i-1)^{a_i}} G_{1,1}^{1,1}\left[\begin{matrix}1-(a_i+b_i)\\0\end{matrix}\middle| Bx\right] \quad (34)$$

Substituting (8) and (34) in (33), and applying the definition of Meijer's G-function, we get

$$f_{h_{tp_i}}(x) = \frac{a_i^{a_i}\rho_i^2 \exp\left(\frac{-s_i^2}{2\sigma_i^2}\right) x^{a_i-1}}{\beta(a_i,b_i)(b_i-1)^{a_i} A_i^{\rho_i^2}} \sum_{j=0}^{\infty} \frac{1}{(j!)^2}\left(\frac{s_i^2\, w_{z_{\mathrm{eq_i}}}^2}{8\sigma_i^4}\right)^j \left(\frac{1}{2\pi\jmath}\int_{\mathcal{L}} \Gamma(-u)\Gamma((a_i+b_i)+u)\,(B_i x)^u\, du\right) I_1 \quad (35)$$

where $I_1 = \int_0^{A_i} h_{p_i}^{\rho_i^2-a_i-u_i-1}(\ln\frac{A_i}{h_{p_i}})^j dh_{p_i}$. Substituting $\log\frac{A_i}{h_{p_i}} = t$, we get $I_1 = A_i^{\rho_i^2-a_i-u_i}\int_0^\infty e^{-(\rho_i^2-a_i-u_i)t}t^j dt = A_i^{\rho_i^2-a_i-u_i}\frac{\Gamma(1+j)}{(\rho_i^2-a_i-u_i)^{1+j}} = A_i^{\rho_i^2-a_i-u_i}\frac{\Gamma(1+j)[\Gamma(\rho_i^2-a_i-u_i)]^{1+j}}{[\Gamma(1+\rho_i^2-a_i-u_i)]^{1+j}}$. Thus, using I_1 in (35) and applying the definition of Meijer G-function, we get the combine PDF of $\mathcal{F}$-turbulence with the non-zero boresight pointing error

$$f_{h_{tp_i}}(x) = \frac{a_i^{a_i}\rho_i^2 \exp\left(\frac{-s_i^2}{2\sigma_i^2}\right)}{A_i^{a_i}\beta(a_i,b_i)(b_i-1)^{a_i}} \sum_{j=0}^{\infty} \frac{1}{j!}\left(\frac{s_i^2\, w_{z_{\mathrm{eq_i}}}^2}{8\sigma_i^4}\right)^j x^{a_i-1} G_{2+j,2+j}^{2+j,1}\left[\begin{matrix}1-a_i-b_i, \{1+\rho_i^2-a_i\}_0^{j+1}\\ 0, \{\rho_i^2-a_i\}_0^{j+1}\end{matrix}\middle| \frac{Bx}{A_i}\right] \quad (36)$$

Note that (36) generalizes the result presented in [28] for zero boresight model.

Similarly, we apply the product distribution of two random variables in $h_i = h_{tp_i} h_{f_i}$ to get the PDF of the combined channel $f_{h_i}(x)$. Using the transformation on $\gamma_i = \bar{\gamma}_i|h_i|^2$, we get the PDF of SNR for the combined channel in (9). We use (9) in $F_{\gamma_i}^{\mathrm{LR}}(\gamma) = \int_0^\gamma f_{\gamma_i}^{\mathrm{LR}}(\gamma)d\gamma$ to derive the CDF of SNR for the combined channel given in (10), which concludes the proof of Lemma 1.

Appendix B
Theorem 1 (Long-Range and Multihop)

First, we use (9) in (12) and substitute $\sqrt{\gamma} = t$ to get the u-th moment of SNR as:

$$\mathbb{E}[\gamma_i^u] = \frac{a_i^{a_i} z_i^{k_i}\rho_i^2 \exp\left(\frac{-s_i^2}{2\sigma_i^2}\right)}{(A_i\sqrt{\bar{\gamma}_i})^{a_i}\beta(a_i,b_i)(b_i-1)^{a_i}} \sum_{j=0}^{\infty} \frac{1}{j!}\left(\frac{s_i^2\, w_{z_{\mathrm{eq_i}}}^2}{8\sigma_i^4}\right)^j \int_0^\infty t^{2u\frac{\phi_i}{N}+a_i-1} G_{2+j+k_i,2+j+k_i}^{2+j+k_i,1}\left[\begin{matrix}1-a_i-b_i, \{1+\rho_i^2-a_i\}_0^{j+1}, \{1+z_i-a_i\}_1^{k_i}\\ 0, \{\rho_i^2-a_i\}_0^{j+1}, \{z_i-a_i\}_1^{k_i}\end{matrix}\middle| \frac{B_i}{A_i\sqrt{\bar{\gamma}_i}}t\right] dt \quad (37)$$

Using the identity [46], Eq. 07.34.21.0009.01] in (37), we get

$$\mathbb{E}[\gamma_i^u] = \frac{a_i^{a_i} z_i^{k_i}\rho_i^2 \exp\left(\frac{-s_i^2}{2\sigma_i^2}\right)}{(A_i\sqrt{\bar{\gamma}_i})^{a_i}\beta(a_i,b_i)(b_i-1)^{a_i}} \sum_{j=0}^{\infty} \frac{1}{j!}\left(\frac{s_i^2\, w_{z_{\mathrm{eq_i}}}^2}{8\sigma_i^4}\right)^j \frac{\left[\Gamma(\rho_i^2+2\frac{\phi_i}{N}u)\right]^{j+1}\left[\Gamma(z_i+2\frac{\phi_i}{N}u)\right]^{k_i}\Gamma(a_i+2\frac{\phi_i}{N}u)\Gamma(b_i-2\frac{\phi_i}{N}u)}{\left[\Gamma\left(1+\rho_i^2+2\frac{\phi_i}{N}u\right)\right]^{j+1}\left[\Gamma\left(1+z_i+2\frac{\phi_i}{N}u\right)\right]^{k_i}} \left(\frac{B_i}{A_i\sqrt{\bar{\gamma}_i}}\right)^{-2u\frac{\phi_i}{N}-a_i} \quad (38)$$

Substituting (38) in (11), applying the definition of Fox's H-function and using the transformation on $\gamma_i = \bar{\gamma}_i|h_i|^2$, we get the PDF of SNR for long-range multihop transmission in (13). Integrating the derived PDF $F_{\gamma_i}^{\mathrm{LR}}(\gamma) = \int_0^\gamma f_{\gamma_i}^{\mathrm{LR}}(\gamma)d\gamma$ with the standard mathematical procedure, we get the CDF of end-to-end SNR in (14).

Appendix C
Lemma 2 (Short-Range and Single-Hop)

Using the product distribution in $h_{fp_i} = h_{f_i}h_{p_i}$ for the joint PDF of the foggy channel and generalized pointing errors, we represent

$$f_{h_{fp_i}}(x) = \int_{h_{fp_i}/A_i}^1 \frac{1}{|h_{f_i}|} f_{h_{p_i}}(x/h_{f_i}) f_{h_{f_i}}(h_{f_i}) dh_{f_i} \quad (39)$$

Substituting (5) and (8) in (39), we get

$$f_{h_{fp_i}}(x) = \frac{z_i^{k_i}\rho_i^2 \exp\left(\frac{-s_i^2}{2\sigma_i^2}\right)}{\Gamma(k_i)A_i^{\rho_i^2}} \sum_{j=0}^{\infty} \frac{1}{(j!)^2}\left(\frac{s_i^2\, w_{z_{\mathrm{eq_i}}}^2}{8\sigma_i^4}\right)^j x^{\rho_i^2-1} \int_{h_{fp_i}/A_i}^1 h_{f_i}^{m-1}\left(\log\frac{1}{h_{f_i}}\right)^{k_i-1}\left(\ln\frac{A_i h_{f_i}}{x}\right)^j dh_{f_i} \quad (40)$$

where $m_i = z_i - \rho_i^2$. Substituting $\log(1/h_{f_i}) = t$ and using binomial expansion $(1-x)^n = \sum_{j=0}^n \binom{n}{j}(1)^{n-j}(-x)^j$ in (40), and using the definition incomplete Gamma function, we get

$$f_{h_{fp_i}}(x) = \frac{z_i^{k_i}\rho_i^2 \exp\left(\frac{-s_i^2}{2\sigma_i^2}\right)}{\Gamma(k_i)A_i^{\rho_i^2}} \sum_{j=0}^{\infty} \frac{1}{(j!)^2}\left(\frac{s_i^2\, w_{z_{\mathrm{eq_i}}}^2}{8\sigma_i^4}\right)^j x^{\rho_i^2-1}\sum_{n=0}^{j}\binom{j}{n}(-1)^n\left(\ln\frac{A_i}{x}\right)^{j-n} m_i^{-n-k_i} \left[\Gamma(n+k_i) - \Gamma\left(n+k_i, m_i\ln\frac{A_i}{x}\right)\right] \quad (41)$$

Using the transformation $\gamma_i = |h_{fp_i}|^2\bar{\gamma}_i$ in (41), we get the PDF of SNR for OWC system over the foggy channel with generalized pointing errors in (22). The CDF of SNR for foggy channel with generalized pointing errors can be obtained using (22) in $F_{\gamma_i}^{\mathrm{SR}}(\gamma) = \int_0^\gamma f_{\gamma_i}^{\mathrm{SR}}(\gamma)d\gamma$, which results into (23).

Appendix D Theorem 2 (Short-Range and Multihop)

Using (22) in (12) and substituting $m_i \ln \frac{A_i\sqrt{\bar{\gamma}_i}}{\sqrt{\gamma}} = t$ and $d\gamma = -\frac{2}{m_i}A_i^2\bar{\gamma}_i \exp(-\frac{2}{m_i}t)dt$ and applying the series expansion of incomplete Gamma function $\Gamma(a,t) \triangleq (a-1)!e^{-t}\sum_{l=0}^{a-1}\frac{t^l}{l!}$[42], we get

$$\mathbb{E}[\gamma_i^u] = \frac{z_i^{k_i}\rho_i^2 \exp\left(\frac{-s_i^2}{2\sigma_i^2}\right)}{m_i^{j+k_i+1}\Gamma(k_i)}(A_i^2\bar{\gamma}_i)^{u\frac{\phi_i}{N}}\sum_{j=0}^{\infty}\frac{1}{(j!)^2}\left(\frac{s_i^2\, w_{z_{\mathrm{eq_i}}}^2}{8\sigma_i^4}\right)^j$$
$$\sum_{n=0}^{j}\binom{j}{n}(-1)^n\Bigg[\Gamma(n+k_i)\int_0^\infty t^{j-n}$$
$$\exp\left(-\left(2u\frac{\phi_i}{m_iN}+\frac{\rho_i^2}{m_i}\right)t\right)dt-(n+k-1)!$$
$$\sum_{l=0}^{n+k-1}\frac{1}{l!}\int_0^\infty t^{j-n+l}\exp\left(-\left(2u\frac{\phi_i}{m_iN}+\frac{\rho_i^2}{m_i}+1\right)t\right)dt\Bigg] \tag{42}$$

To represent the u-th moment in terms of Gamma functions, we solve (42) using the identity $\int_0^\infty t^a \exp(-bt)dt = b^{-a-1}\Gamma(a+1)$ and $\frac{1}{u} = \frac{\Gamma(u)}{\Gamma(1+u)}$ as:

$$\mathbb{E}[\gamma_i^u] = \frac{z_i^{k_i}\rho_i^2 \exp\left(\frac{-s_i^2}{2\sigma_i^2}\right)}{m_i^{j+k_i+1}\Gamma(k_i)}(A_i^2\bar{\gamma}_i)^{u\frac{\phi_i}{N}}\sum_{j=0}^{\infty}\frac{1}{(j!)^2}\left(\frac{s_i^2\, w_{z_{\mathrm{eq_i}}}^2}{8\sigma_i^4}\right)^j$$
$$\sum_{n=0}^{j}\binom{j}{n}(-1)^n\Bigg[\Gamma(n+k_i)\Gamma(1+j-n)$$
$$\left(\frac{\Gamma\left(\frac{\rho_i^2}{m_i}+\frac{2\phi_i}{m_iN}u\right)}{\Gamma\left(1+\frac{\rho_i^2}{m_i}+\frac{2\phi_i}{m_iN}u\right)}\right)^{n-j-1}-(n+k-1)!$$
$$\sum_{l=0}^{n+k-1}\frac{1}{l!}\Gamma(1+j-n+l)\left(\frac{\Gamma\left(1+\frac{\rho_i^2}{m_i}+\frac{2\phi_i}{m_iN}u\right)}{\Gamma\left(2+\frac{\rho_i^2}{m_i}+\frac{2\phi_i}{m_iN}u\right)}\right)^{n-j-l-1}\Bigg] \tag{43}$$

Thus, invoking (43) in (11) and applying the definitions of Fox's H-function, we get PDF of SNR for multihop transmission in (24). The CDF is driven by applying standard mathematical steps in $F_{\gamma_i}^{\mathrm{SR}}(\gamma) = \int_0^\gamma f_{\gamma_i}^{\mathrm{SR}}(\gamma)d\gamma$ to get (25), which concludes the proof of Theorem 2.

References

[1] M. A. Khalighi and M. Uysal, "Survey on free space optical communication: A communication theory perspective," *IEEE Commun. Surv. Tut.*, vol. 16, no. 4, pp. 2231–2258, Oct.–Dec. 2014.

[2] H. Kaushal and G. Kaddoum, "Optical communication in space: Challenges and mitigation techniques," *IEEE Commun. Surv. Tut.*, vol. 19, no. 1, pp. 57–96, Jan.–Mar. 2017.

[3] M. Alzenad, M. Z. Shakir, H. Yanikomeroglu, and M.-S. Alouini, "FSO-based vertical backhaul/fronthaul framework for 5G wireless networks," *IEEE Commun. Mag.*, vol. 56, no. 1, pp. 218–224, Jan. 2018.

[4] G. Xu and Z. Song, "Effects of solar scintillation on deep space communications: Challenges and prediction techniques," *IEEE Wireless Commun.*, vol. 26, no. 2, pp. 10–16, Apr. 2019.

[5] M. Aggarwal, P. Garg, and P. Puri, "Dual-hop optical wireless relaying over turbulence channels with pointing error impairments," *J. Lightw. Technol.*, vol. 32, no. 9, pp. 1821–1828, May 2014.

[6] L. Yang, X. Gao, and M.-S. Alouini, "Performance analysis of relay-assisted all-optical FSO networks over strong atmospheric turbulence channels with pointing errors," *J. Lightw. Technol.*, vol. 32, no. 23, pp. 4613–4620, Dec. 2014.

[7] J. Libich, M. Komanec, S. Zvanovec, P. Pesek, W. O. Popoola, and Z. Ghassemlooy, "Experimental verification of an all-optical dual-hop 10 Gbit/s free-space optics link under turbulence regimes," *Opt. Lett.*, vol. 40, no. 3, pp. 391–394, Feb. 2015.

[8] E. Zedini, H. Soury, and M.-S. Alouini, "Dual-hop FSO transmission systems over Gamma–Gamma turbulence with pointing errors," *IEEE Trans. Wireless Commun.*, vol. 16, no. 2, pp. 784–796, Feb. 2017.

[9] T. A. Tsiftsis, H. G. Sandalidis, G. K. Karagiannidis, and N. C. Sagias, "Multihop free-space optical communications over strong turbulence channels," in *Proc. IEEE Int. Conf. Commun.*, 2006, pp. 2755–2759.

[10] S. M. Aghajanzadeh and M. Uysal, "Multi-hop coherent free-space optical communications over atmospheric turbulence channels," *IEEE Trans. Commun.*, vol. 59, no. 6, pp. 1657–1663, Jun. 2011.

[11] M. Safari, M. M. Rad, and M. Uysal, "Multi-hop relaying over the atmospheric Poisson channel: Outage analysis and optimization," *IEEE Trans. Commun.*, vol. 60, no. 3, pp. 817–829, Mar. 2012.

[12] M. A. Kashani and M. Uysal, "Outage performance and diversity gain analysis of free-space optical multi-hop parallel relaying," *J. Opt. Commun. Netw.*, vol. 5, no. 8, pp. 901–909, Aug. 2013.

[13] P. Wang, T. Cao, L. Guo, R. Wang, and Y. Yang, "Performance analysis of multihop parallel free-space optical systems over exponentiated Weibull fading channels," *IEEE Photon. J.*, vol. 7, no. 1, Feb. 2015, Art. no. 7900715.

[14] P. Wang et al., "Performance analysis for relay-aided multihop BPPM FSO communication system over exponentiated Weibull fading channels with pointing error impairments," *IEEE Photon. J.*, vol. 7, no. 4, Aug. 2015, Art. no. 4600420.

[15] P. Wang et al., "Multihop FSO over exponentiated Weibull fading channels with nonzero boresight pointing errors," *IEEE Photon. Technol. Lett.*, vol. 28, no. 16, pp. 1747–1750, Aug. 2016.

[16] C. B. Issaid, K.-H. Park, and M.-S. Alouini, "A generic simulation approach for the fast and accurate estimation of the outage probability of single hop and multihop FSO links subject to generalized pointing errors," *IEEE Trans. Wireless Commun.*, vol. 16, no. 10, pp. 6822–6837, Oct. 2017.

[17] C. K. Datsikas, K. P. Peppas, N. C. Sagias, and G. S. Tombras, "Serial free-space optical relaying communications over Gamma-Gamma atmospheric turbulence channels," *J. Opt. Commun. Netw.*, vol. 2, no. 8, pp. 576–586, 2010.

[18] E. Zedini and M.-S. Alouini, "Multihop relaying over IM/DD FSO systems with pointing errors," *J. Lightw. Technol.*, vol. 33, no. 23, pp. 5007–5015, Dec. 2015.

[19] E. Zedini and M.-S. Alouini, "On the performance of multihop heterodyne FSO systems with pointing errors," *IEEE Photon. J.*, vol. 7, no. 2, Apr. 2015, Art. no. 7901110.

[20] X. Tang, Z. Wang, Z. Xu, and Z. Ghassemlooy, "Multihop free-space optical communications over turbulence channels with pointing errors using heterodyne detection," *J. Lightw. Technol.*, vol. 32, no. 15, pp. 2597–2604, Aug. 2014.

[21] W. G. Alheadary, K.-H. Park, and M.-S. Alouini, "Performance analysis of multi-hop heterodyne FSO systems over Malaga turbulent channels with pointing error using mixture gamma distribution," in *Proc. IEEE 85th Veh. Technol. Conf.*, 2017, pp. 1–5.

[22] W. G. Alheadary, K.-H. Park, and M.-S. Alouini, "BER analysis of multi-hop heterodyne FSO systems with fixed gain relays over general Malaga turbulence channels," in *Proc. 13th Int. Wireless Commun. Mobile Comput. Conf.*, 2017, pp. 1172–1177.

[23] W. Pang et al., "Performance analysis for multi-hop FSO communication system over M distribution with pointing errors," in *Proc. 19th Int. Conf. Opt. Commun. Netw.*, 2021, pp. 1–3.

[24] B. Ashrafzadeh, A. Zaimbashi, E. Soleirnani-Nasab, and M. Uysal, "On the performance of multi-hop free space optical cooperative systems," in *Proc. IEEE Glob. Commun. Conf.*, 2018, pp. 1–6.

[25] B. Ashrafzadeh, A. Zaimbashi, E. Soleimani-Nasab, and M. Uysal, "Unified performance analysis of multi-hop FSO systems over double generalized gamma turbulence channels with pointing errors," *IEEE Trans. Wireless Commun.*, vol. 19, no. 11, pp. 7732–7746, Nov. 2020.

[26] G. Karagiannidis, T. Tsiftsis, and R. Mallik, "Bounds for multihop relayed communications in Nakagami-m fading," *IEEE Trans. Commun.*, vol. 54, no. 1, pp. 18–22, Jan. 2006.

[27] K. P. Peppas, G. C. Alexandropoulos, E. D. Xenos, and A. Maras, "The Fischer-Snedecor $\mathcal{F}$-distribution model for turbulence-induced fading in free-space optical systems," *J. Lightw. Technol.*, vol. 38, no. 6, pp. 1286–1295, Mar. 2020.

[28] O. S. Badarneh, R. Derbas, F. S. Almehmadi, F. El Bouanani, and S. Muhaidat, "Performance analysis of FSO communications over F turbulence channels with pointing errors," *IEEE Commun. Lett.*, vol. 25, no. 3, pp. 926–930, Mar. 2021.

[29] O. S. Badarneh and R. Mesleh, "Diversity analysis of simultaneous mmWave and free-space-optical transmission over $\mathcal{F}$-distribution channel models," *J. Opt. Commun. Netw.*, vol. 12, no. 11, pp. 324–334, Nov. 2020.

[30] L. Han, Y. Wang, X. Liu, and B. Li, "Secrecy performance of FSO using HD and IM/DD detection technique over $\mathcal{F}$-distribution turbulence channel with pointing error," *IEEE Wireless Commun. Lett.*, vol. 10, no. 10, pp. 2245–2248, Oct. 2021.

[31] W. M. R. Shakir and M.-S. Alouini, "Secrecy performance analysis of parallel FSO/mm-wave system over unified Fisher-Snedecor channels," *IEEE Photon. J.*, vol. 14, no. 2, Apr. 2022, Art. no. 7317013.

[32] J. Ding, X. Xie, L. Tan, J. Ma, and D. Kang, "Dual-hop RF/FSO systems over $\kappa - \mu$ shadowed and Fisher-Snedecor $\mathcal{F}$ fading channels with non-zero boresight pointing errors," *J. Lightw. Technol.*, vol. 40, no. 12, pp. 4057–4057, Jun. 2022.

[33] M. Khan, M. Awan, E. Leitgeb, F. Nadeem, and I. Hussain, "Selecting a distribution function for optical attenuation in dense continental fog conditions," in *Proc. Int. Conf. Emerg. Technol.*, 2009, pp. 142–147.

[34] M. A. Esmail, H. Fathallah, and M.-S. Alouini, "Outdoor FSO communications under fog: Attenuation modeling and performance evaluation," *IEEE Photon. J.*, vol. 8, no. 4, Aug. 2016, Art. no. 7905622.

[35] M. A. Esmail, H. Fathallah, and M.-S. Alouini, "On the performance of optical wireless links over random foggy channels," *IEEE Access*, vol. 5, pp. 2894–2903, 2017.

[36] M. A. Esmail, H. Fathallah, and M.-S. Alouini, "Outage probability analysis of FSO links over foggy channel," *IEEE Photon. J.*, vol. 9, no. 2, Apr. 2017, Art. no. 7902312.

[37] Z. Rahman, S. M. Zafaruddin, and V. K. Chaubey, "Performance of opportunistic beam selection for OWC system under foggy channel with pointing error," *IEEE Commun. Lett.*, vol. 24, no. 9, pp. 2029–2033, Sep. 2020.

[38] Z. Rahman, T. N. Shah, S. M. Zafaruddin, and V. K. Chaubey, "Performance of dual-hop relaying for OWC system over foggy channel with pointing errors and atmospheric turbulence," *IEEE Trans. Veh. Technol.*, vol. 71, no. 4, pp. 3776–3791, Apr. 2022.

[39] A. A. Farid and S. Hranilovic, "Outage capacity optimization for free-space optical links with pointing errors," *J. Lightw. Technol.*, vol. 25, no. 7, pp. 1702–1710, Jul. 2007.

[40] M. O. Hasna and M.-S. Alouini, "Outage probability of multihop transmission over Nakagami fading channels," *IEEE Commun. Lett.*, vol. 7, no. 5, pp. 216–218, May 2003.

[41] K.-J. Jung, S. S. Nam, M.-S. Alouini, and Y.-C. Ko, "Unified finite series approximation of FSO performance over strong turbulence combined with various pointing error conditions," *IEEE Trans. Commun.*, vol. 68, no. 10, pp. 6413–6425, Oct. 2020.

[42] D. Zwillinger, *Table of Integrals, Series, and Products*. Amsterdam, The Netherlands: Elsevier, 2014.

[43] V. K. Chapala and S. M. Zafaruddin, "Unified performance analysis of reconfigurable intelligent surface empowered free-space optical communications," *IEEE Trans. Commun.*, vol. 70, no. 4, pp. 2575–2592, Apr. 2022.

[44] P. Bhardwaj and S. M. Zafaruddin, "On the performance of multihop THz 842 wireless system over mixed channel fading with shadowing and antenna 843 misalignment," 2021. [Online]. Available online: http://arxiv.org/pdf/2110.15952.pdf

[45] H. M. Srivastava and H. L. Manocha, *A Treatise on Generating Functions, Ellis Horwood series in mathematics and its applications*, E. Horwood; New York, NY, USA: Halsted Press, 1984.

[46] Wolfram, "The Wolfram functions site," Internet, 2001. [Online]. Available: http://functions.wolfram.com

[47] A. Kilbas, *Analytical Methods and Special Functions, H-Transforms: Theory and Applications*. New York, NY, USA: Taylor and Francis, 2004.

[48] B. Ashrafzadeh, E. Soleimani-Nasab, M. Kamandar, and M. Uysal, "A framework on the performance analysis of dual-hop mixed FSO-RF cooperative systems," *IEEE Trans. Commun.*, vol. 67, no. 7, pp. 4939–4954, Jul. 2019.

[49] Z. Rahman, S. M. Zafaruddin, and V. K. Chaubey, "Performance of opportunistic receiver beam selection in multiaperture OWC systems over foggy channels," *IEEE Syst. J.*, vol. 14, no. 3, pp. 4036–4046, Sep. 2020.

[50] P. Mittal and K. Gupta, "An integral involving generalized function of two variables," *Proc. Indian Acad. Sci.*, vol. 75, no. 9, pp. 117–123, 1972.

[51] A. P. Prudnikov, Y. A. Brychkov, and O. I. Marichev, *Integrals and Series: More Special Functions*, vol. 3. New York, NY, USA: Gordon and Breach Science Publishers, 1998.